JOURNAL OF VIROLOGY, June 2009, p. 6048–6066 Vol. 83, No. 12
0022-538X/09/$08.00+0 doi:10.1128/JVI.00012-09

Improved Adenovirus Type 5 Vector-Mediated Transduction of Resistant Cells by Piggybacking on Coxsackie B-Adenovirus Receptor-Pseudotyped Baculovirus▽

Ophélia Granio,[1]† Marine Porcherot,[1]† Stéphanie Corjon,[1] Kuntida Kitidee,[1,2] Petra Henning,[3] Assia Eljaafari,[4] Andrea Cimarelli,[5] Leif Lindholm,[6] Pierre Miossec,[4] Pierre Boulanger,[1,7] and Saw-See Hong[1]*

Université Lyon I, Laboratoire de Virologie et Pathologie Humaine, CNRS FRE 3011, Faculté de Médecine Claude Bernard and IFR Laennec, 7, rue Guillaume Paradin, 69372 Lyon, France[1]; Division of Clinical Immunology, Faculty of Associated Medical Sciences, Chiang Mai University, Chiang Mai, 50200 Thailand[2]; Institute for Biomedicine, Department of Microbiology and Immunology, University of Göteborg, P.O. Box 435, SE 40530 Göteborg, Sweden[3]; Department of Immunology and Rheumatology, Hôpital Edouard Herriot, 69437 Lyon, France[4]; LaboRetro, Department of Human Virology, Ecole Normale Supérieure de Lyon, INSERM U 758, Université Lyon I, IFR128 BioSciences Lyon-Gerland, Lyon-Biopole, 46, Allée d'Italie, 69364 Lyon, France[5]; Got-A-Gene AB, Östra Kyviksvägen 18, SE 42930 Kullavik, Sweden[6]; and Laboratoire de Virologie Médicale, Centre de Biologie Est, Hospices Civils de Lyon, 59, Boulevard Pinel, 69677 Bron, France[7]

Received 5 January 2009/Accepted 27 March 2009

Taking advantage of the wide tropism of baculoviruses (BVs), we constructed a recombinant BV (BV^{CAR}) pseudotyped with human coxsackie B-adenovirus receptor (CAR), the high-affinity attachment receptor for adenovirus type 5 (Ad5), and used the strategy of piggybacking Ad5-green fluorescent protein (Ad5GFP) vector on BV^{CAR} to transduce various cells refractory to Ad5 infection. We found that transduction of all cells tested, including human primary cells and cancer cell lines, was significantly improved using the BV^{CAR}-Ad5GFP biviral complex compared to that obtained with Ad5GFP or BV^{CAR}GFP alone. We determined the optimal conditions for the formation of the complex and found that a high level of BV^{CAR}-Ad5GFP-mediated transduction occurred at relatively low adenovirus vector doses, compared with transduction by Ad5GFP alone. The increase in transduction was dependent on the direct coupling of BV^{CAR} to Ad5GFP via CAR-fiber knob interaction, and the cell attachment of the BV^{CAR}-Ad5GFP complex was mediated by the baculoviral envelope glycoprotein gp64. Analysis of the virus-cell binding reaction indicated that the presence of BV^{CAR} in the complex provided kinetic benefits to Ad5GFP compared to the effects with Ad5GFP alone. The endocytic pathway of BV^{CAR}-Ad5GFP did not require Ad5 penton base RGD-integrin interaction. Biodistribution of BV^{CAR}-Ad5Luc complex in vivo was studied by intravenous administration to nude BALB/c mice and compared to Ad5Luc injected alone. No significant difference in viscerotropism was found between the two inocula, and the liver remained the preferred localization. In vitro, coagulation factor X drastically increased the Ad5GFP-mediated transduction of CAR-negative cells but had no effect on the efficiency of transduction by the BV^{CAR}-Ad5GFP complex. Various situations in vitro or ex vivo in which our BV^{CAR}-Ad5 duo could be advantageously used as gene transfer biviral vector are discussed.

Adenoviruses (Ads) are extensively used today as gene transfer vectors for in vitro, ex vivo, and in vivo gene transfer protocols (reviewed in reference 65). Cell entry of human Ad type 5 (Ad5), the serotype most widely used as a gene vector, occurs most efficiently by the receptor-mediated endocytosis pathway (reviewed in references 64 and 65), via the coxsackievirus B-adenovirus receptor (CAR) (3, 77) and αvβ3/αvβ5 integrins (84, 85), although alternative receptors have been described (11, 12, 14, 27). Cell surface expression of CAR differs with different cell types, and this represents one of the major determinants of the efficiency of Ad5-mediated transduction (43). The ubiquitous nature of CAR is responsible for transduction of nontarget tissues by Ad vectors. Paradoxically, many target cells such as dermal fibroblasts, synoviocytes, mesenchymal stem cells (MSCs), peripheral blood mononuclear cells (PBMCs), and dendritic cells (DCs), express no or very low levels of CAR at their surface and are relatively resistant to Ad transduction (14, 15, 19). Much work has been done with different strategies to promote the entry of Ad5 into CAR-defective cells. These strategies include (i) the genetic modification of Ad capsid proteins to carry cell ligands (2, 15, 20, 28, 49, 50), (ii) pseudotyping Ad5 vectors with fibers from other serotypes (13, 57, 74, 86), (iii) using bispecific adapters or peptides (25, 40), (iv) chemical modification of Ad (9, 42), and (v) tethering on nanoparticles (7). The limitations to these strategies are that modifications of the Ad capsid are susceptible to negatively affecting the virus growth or viability, due to an alteration of virion assembly,

* Corresponding author. Mailing address: Laboratoire de Virologie et Pathologie Humaine, CNRS FRE 3011, Faculté de Médecine and IFR Laennec, 7, rue Guillaume Paradin, 69372 Lyon, France. Phone: (33) 4 7877 8621. Fax: (33) 4 7877 8751. E-mail: sawsee.hong@sante.univ-lyon1.fr.
† These authors contributed equally to this work.
▽ Published ahead of print on 8 April 2009.

stability, the viral uncoating process, and/or intracellular trafficking (13, 51).

Other viruses which are gaining popularity as gene transfer vectors are the baculoviruses (BVs). *Autographa californica* multiple nucleopolyhedrosis virus (AcMNPV) is an insect virus with a large double-stranded DNA genome packaged in a membrane-enveloped, rod-shaped protein capsid (70). Since the 1980s, the BV-insect cell expression system has been highly exploited for the production of recombinant proteins. In the mid-1990s, it was shown that recombinant BVs carrying reporter genes under cytomegalovirus (CMV) or retroviral Rous sarcoma virus promoter efficiently expressed reporter genes in mammalian cells (6, 22, 38, 41, 44, 69), as well as in avian cells (72) and fish cells (45). Since then, BVs have been reported to transduce numerous cells originating from species as various as humans, bovines, and fish (8, 32, 41, 73). As gene transfer vectors, BVs have been found to be rapidly inactivated by human serum complement (23), but exposing decay-accelerating factor (DAF) at the surface of BV by fusion with the baculoviral envelope glycoprotein can overcome this inactivation (33). BVs also have a good biosafety profile due to their incapacity to replicate in mammalian cells (31).

Taking advantage of the ability of BVs to transduce a large repertoire of cells of invertebrate and vertebrate origins, including human primary cells, we investigated whether a recombinant AcMNPV could act as a carrier or macroadapter for Ad5 vectors to enter Ad5-refractory cells. To this aim, we pseudotyped AcMNPV virions with the high-affinity receptor for Ad5, the human CAR glycoprotein (BV^{CAR}), to enable the formation of complexes between vector particles of BV^{CAR} and Ad5-green fluorescent protein (Ad5GFP) mediated by Ad5 fiber and CAR interaction. We found that transduction of cell lines which were poorly permissive to Ad5, including human cancer cells and primary cells, was significantly improved using this strategy of piggybacking Ad5 vector on BV^{CAR}. More importantly, the increase in BV^{CAR}-Ad5-mediated transduction was obtained with a low range of Ad5 inputs, i.e., at multiplicities of infection (MOI) of less than 50 Ad5 vector particles per cell. We also found that the cell transduction enhancement observed with BV^{CAR}-Ad5 required the direct coupling of Ad5 to BV^{CAR} via fiber-CAR binding and that the cell attachment of the complex was mediated by the baculoviral envelope glycoprotein gp64. Kinetic analysis of virus-cell binding showed that the presence of BV^{CAR} in the complex was beneficial to Ad5 vector, not only in terms of tropism but also in terms of number of cell-bound virions and rate of cell attachment. In addition, the endocytic pathway of BV^{CAR}-Ad5 did not require Ad5 penton base RGD-integrin interaction. When administered in vivo to nude BALB/c mice, BV^{CAR}-Ad5 complex showed the same biodistribution as that of control Ad5 vector injected alone. In vitro, transduction of CAR-negative cells by BV^{CAR}-Ad5 was insensitive to coagulation factor X (FX), in contrast to Ad5 vector alone.

Our novel strategy of gene delivery using the BV^{CAR}-Ad5 duo could be advantageously applied to various situations in vitro or ex vivo, e.g., for transducing Ad5-refractory cells when Ad5 capsid modifications cannot be envisaged, when oncolytic Ads need to be delivered to tumors via nonpermissive cell carriers belonging to the immune system, or when the simultaneous delivery of two transgenes by two separate vectors might be beneficial in terms of timing and/or level of cellular expression of the transgene products.

MATERIALS AND METHODS

Cells. (i) Cell lines. *Spodoptera frugiperda* (Sf9) cells were maintained as monolayers at 28°C in Grace's insect medium supplemented with 10% fetal bovine serum (FBS) and antibiotics (Invitrogen). Chinese hamster ovarian cells (CHO), human embryonic kidney cells (HEK-293), human rhabdomyosarcoma cells (RD), human ovarian carcinoma cells (SKOV3), and human breast carcinoma cells (SKBR3) were purchased from the American Type Culture Collection (ATCC, Manassas, VA) and grown in Iscove's medium supplemented with 10% FBS and 50 mg/ml gentamicin (Invitrogen). CAR-expressing CHO cells (CHO-CAR) were obtained from J. Bergelson (3).

(ii) Primary cells. Human synoviocytes were obtained from synovial tissue from rheumatoid arthritis patients undergoing joint surgery. Human dermal fibroblasts were obtained from the skin of a patient undergoing joint surgery for osteoarthritis. Both synoviocytes and dermal fibroblasts were isolated by enzyme digestion and cultured in Dulbecco modified Eagle medium supplemented with 10% FBS and antibiotics (76) and were used between passages 4 and 9. Human MSC cultures were established using the French National protocol of the SFGM-TC Society. Briefly, bone marrow aspirates were obtained from the posterior iliac crest of healthy donors after their consent was given, and bone marrow mononuclear cells were isolated by Ficoll density gradient centrifugation (Lymphoprep; Abcys, Veyrier-du-Lac, France). Mononuclear cells (2.5×10^5/ml) were seeded in α-minimal essential medium (Gibco BRL, Paisley, United Kingdom) supplemented with 10% FBS, 2 mM L-glutamine, and 100 U/ml penicillin-streptomycin. Cells were allowed to adhere for 48 h followed by the removal of nonadherent cells. Medium and nonadherent cells were removed every 3 days thereafter. When culture was confluent, adherent cells were detached using trypsin and reseeded into a new flask, for expansion. At the third passage, MSCs were identified by immunophenotypic criteria based on the expression of CD73, CD90, and CD105 and the absence of expression of CD45, CD34, CD14, CD19, and HLA-DR before use (46). Monocyte-derived human DCs were obtained as follows. Immature DCs were differentiated from primary monocytes obtained from PBMCs of healthy donors upon incubation for 4 to 6 days with 100 ng/ml of interleukin 4 and granulocyte-macrophage colony-stimulating factor, as previously described (16). Both interleukin 4 and granulocyte-macrophage colony-stimulating factor were from R&D. Cells were maintained in complete RPMI 1640 medium supplemented with 10% fetal calf serum (BioWest). All experiments using human primary cells were performed in accordance with ethical guidelines and regulations and received approval from the Institutional Review board of the Laennec School of Medicine.

Human Ads and BVs. Replication-deficient Ad5 vectors (E1 deleted) expressing GFP (Ad5GFP) under the CMV promoter were propagated in HEK-293 cells. The penton base mutant Ad5EGD-GFP, encoding GFP and carrying an RGD-to-EGD alteration at position 340 in the penton base coding sequence, has been described elsewhere (13, 83). The fiber mutant Ad5GFP-R7ΔKnob, carrying a short shafted fiber with seven repeats (R7) and complete deletion of the knob (ΔKnob), has been described in detail in previous studies (20, 28, 50, 51). Ad5Luc, expressing the luciferase gene in the deleted E3 region of the Ad5 genome under the control of the simian virus 40 promoter, was obtained from Frank Graham (University of Ontario, Hamilton, Ontario, Canada) and described in previous studies (27, 56). Ad stocks were purified by CsCl gradient ultracentrifugation by conventional methods (13). The recombinant AcMNPV expressing CAR (BV^{CAR}) was constructed by cloning the human full-length CAR gene DNA into the NheI and KpnI cloning sites of pBlueBac (Invitrogen) downstream to the polyhedrin promoter, as described in previous studies (36, 37). The CAR gene DNA was isolated by digestion of the pcDNA-hCAR1 plasmid (obtained from Kerstin Sollerbrant, Karolinska Institutet, Stockholm, Sweden [71]) with NheI and KpnI. The recombinant BV expressing GFP under the CMV promoter (BV-GFP) was kindly provided by Norman Maitland (University of York at Heslington, York, United Kingdom). BV^{CAR} and BV-GFP were propagated by infection of Sf9 cells at a MOI of 1 to 2. Concentrated stocks of recombinant BV were prepared as follows. Infected cell supernatants were harvested at 48 to 60 h postinfection (p.i.), clarified by centrifugation at 2,400 rpm and 4°C for 10 min, and subjected to ultracentrifugation at 28,000 rpm for 1 h at 4°C through a 20% sucrose cushion. The viral pellet was resuspended by gentle shaking in sterile phosphate-buffered saline (PBS) overnight at 4°C, and further purified by isopycnic ultracentrifugation in a linear sucrose-D_2O gradient (10, 34). Gradients (10-ml total volume, 30 to 50% [wt/vol]) were generated from a 50% sucrose solution made in D_2O buffered to pH 7.2 with NaOH and a 30% sucrose solution made in 10 mM Tris-HCl, pH 7.2, 150 mM NaCl, 5.7 mM

Na_2-EDTA. The gradients were centrifuged for 18 h at 28,000 rpm in a Beckman SW41 rotor. Fractions (0.5 ml) were collected from the top, and proteins were analyzed by sodium dodecyl sulfate-polyacrylamide gel electrophoresis (SDS-PAGE) and Western blotting with the required antibodies. Baculovirions pseudotyped with CAR were produced by single infection of Sf9 cells with BV^{CAR} and isolated from infected cell culture supernatant as described above. Infectious titers of BV vector stocks were determined using the plaque assay on Sf9 cells.

Generation of BV^{CAR}- Ad5 complex. The infectivity index, defined as the ratio of infectious virions (determined by the plaque assay method and expressed as PFU per ml) to the total number of physical virus particles per ml (vp/ml), ranged from 1:100 to 1:500 for BVs (80), a value which was about 5- to 20-fold lower than that of Ad5, which was routinely about 1:20 to 1:30. The titer in physical vp of BV and Ad5 vectors was determined by absorbance measurement at 260 nm (A_{260}) of 1-ml samples of SDS-denatured virions (0.1% SDS for 1 min at 56°C) in a 1-cm-path-length cuvette, using the respective formulas A_{260} of $1.0 = 1.1 \times 10^{12}$ vp/ml for Ad5 (genomic DNA = 36 kbp) and A_{260} of $1.0 = 0.3 \times 10^{12}$ vp/ml for BV (genomic DNA = 134 kbp). Infectious titers of concentrated stocks of BV^{CAR} were usually 5×10^9 to 1×10^{10} PFU/ml, and the corresponding physical particle titers ranged between 1×10^{12} and 5×10^{12} vp/ml. Ad5GFP particle titers ranged from 1×10^{12} to 2×10^{12} vp/ml, with infectious titers between 2×10^{10} and 5×10^{10} PFU/ml. To generate BV^{CAR}-Ad5GFP complexes with different virus ratios, we considered only the respective titers in vp/ml. In standard experiments, samples of BV^{CAR} and Ad5GFP virions in 50 mM Tris-HCl (pH 8.0) buffer were mixed and adjusted to a total volume of 20 to 30 μl with the same buffer and then incubated for 1 h at 37°C.

Antibodies and proteins. Monoclonal anti-CAR antibody (clone E1.1 [19]) was obtained from Silvio Hemmi (University of Zürich, Zürich, Switzerland). The monoclonal anti-gp64 antibody clone AcV1 (Santa Cruz Biotechnology, Inc.) was used at a working dilution of 1:50 for immunoelectron microscopy. Mouse monoclonal antibody 7A7 directed against the fiber knob domain has been characterized in a previous study (27). Group-specific antihexon monoclonal antibody 4C3 was provided by W. C. Russell (University of St. Andrews, St. Andrews, Scotland) (29, 55, 66). Rabbit anti-Ad5 virion, anti-penton base, and antifiber were all laboratory made (13, 36, 37, 60). Human coagulation FX was purchased from Haematologic Technologies, Inc. (Essex Junction, VT) and used at the normal adult plasma concentration of 8 μg/ml. Adenoviral capsid proteins, hexon, fiber, and penton (base-plus-fiber) proteins were recovered from the pool of excess soluble Ad5 proteins present in Ad5-infected cell lysates used for vector stock preparations. Capsid proteins were purified to homogeneity according to a three-step procedure including ammonium sulfate precipitation and two chromatographic steps using high-performance liquid chromatography (BioLogic DuoFlow; Bio-Rad), as described in detail in previous studies (5, 58).

Cell transduction assays. Cells for transduction assays were prepared in 24-well plates containing 1×10^5 cells per well. Complexes of BV^{CAR} and Ad5GFP virions (BV^{CAR}-Ad5GFP) were prepared by preincubating appropriate volumes of each virus in a total volume of 300 μl of Dulbecco modified Eagle medium for 1 h at 37°C. The complexes were then added to the cells and incubated for an additional hour at 37°C, after which 200 μl prewarmed medium was added to each well. Cellular expression of GFP was observed at 36 h posttransduction, using an inverted microscope (Axiovert-135; Zeiss, Switzerland). Fluorescence images were taken using an AxioCam digital camera (Zeiss), analyzed using an Axio Vision program, and quantitated by flow cytometry analysis. For quantification, cells were fixed with 2% paraformaldehyde in PBS overnight and rinsed once with PBS and the proportion of GFP-positive cells was determined by fluorescence-activated cell sorting analysis (Dako Galaxy).

Real-time quantitative PCR. DNA was extracted from murine tissues using the QIAamp DNA blood minikit (Qiagen, Courtaboeuf, France). Ad5 genomes were assayed using the following fiber gene primers for real-time PCR (9): GCTACAGTTTCAGTTTTGGCTG (sense) and GTTGTGGCCAGACCAG TCCC (reverse). BV genomes were assayed using the following gp64 gene primers (1): ATGAGCAGACACGCAGCTTTT (sense) and GCTGAATGTG GGCAAAGAGG (reverse). The murine beta-actin gene was used as an internal control, with the following primers: GCTGTGTTCTTGCACTCCTTG (sense) and CGCACGATTTCCCTCTCAGC (reverse). Real-time PCR was performed using a LightCycler 480 (Roche Diagnostics, Meylan, France), and results were expressed as the number of viral genome copies per cell.

Electron microscopy. Virions of BV^{CAR} and BV^{CAR}-Ad5GFP complexes were diluted in 20 μl 0.14 M NaCl, 0.05 M Tris-HCl buffer, pH 8.2 (Tris-buffered saline [TBS]), and adsorbed onto carbon-coated Formvar membranes on grids. The grids were incubated with primary antibody (monoclonal anti-CAR or anti-gp64 antibody) at a dilution of 1:50 in TBS for 1 h at room temperature (RT). After being rinsed with TBS, the grids were postincubated with 20-nm colloidal gold-tagged goat anti-mouse immunoglobulin G (IgG) antibody (British Biocell International Ltd., Cardiff, United Kingdom; diluted to 1:50 in TBS) for 30 min at RT. After being rinsed with TBS, the specimens were negatively stained with 1% uranyl acetate in H_2O for 1 min at RT, rinsed again with TBS, and examined under a JEM 1400 JEOL electron microscope (EM) equipped with an Orius-Gatan digitalized camera (Gatan, Grandchamp, France).

Animal model. All procedures were performed on 5-week-old female BALB/c *nu/nu* mice (Charles River Laboratories, St. Germain sur l'Arbresle, France). Studies involving animals, including housing and care, method of euthanasia, and experimental protocols, were conducted in accordance with a code of practice established by the Experimentation Review Board from the Laennec School of Medicine. These studies were routinely inspected by the Attending Veterinarian to ensure continued compliance with the proposed protocols (63). Mice received intravenously in the tail vein 2×10^{10} vp of Ad5Luc per mouse (control animals) or BV^{CAR}-Ad5Luc complex formed in the ratio of 15 BV^{CAR} to 1 Ad5Luc (2×10^{10} vp of Ad5Luc and 3×10^{11} vp of BV^{CAR} per mouse). At 48 and 96 h after injection, the mice were anesthetized and injected subcutaneously with endotoxin-free luciferin (Luciferin-EF; Promega, Madison, WI) in PBS at 125 mg/kg of body weight, and 10 min later the whole-body bioluminescence was visualized using the NightOWL II LB 983 imaging system (Berthold Technologies GmbH, Bad Wildbad, Germany). After noninvasive whole-body imaging, the animals were sacrificed and the level of luciferase expression was assayed in different organs, using a Lumat LB 9507 luminometer (Berthold), as previously described (25, 27). Results were expressed as relative light units per mg of protein in the respective cell lysates.

RESULTS

Pseudotyping BV with human CAR glycoprotein: qualitative aspects. We constructed a recombinant BV expressing the full-length human CAR glycoprotein (BV^{CAR}) under the control of the polyhedrin promoter and determined whether progeny viruses produced from BV^{CAR}-infected cells carried the CAR glycoprotein on their envelope. Baculovirions released in the culture medium were concentrated by ultracentrifugation on a sucrose cushion and further purified by ultracentrifugation on a linear sucrose density gradient. The fractions at density 1.10 to 1.15 which contained the BV particles were pooled and analyzed by SDS-PAGE and Western blotting using anti-gp64 and anti-CAR antibodies. A discrete band of anti-CAR-reacting protein species migrating at 45 kDa (an apparent molecular mass consistent with that of CAR glycoprotein) was found to be associated with BV^{CAR} virions (Fig. 1a). This band was absent from the control, parental BV vector (AcMNPV-β-Gal expressing bacterial β-galactosidase). Baculovirions were then analyzed by immunoelectron microscopy, after deposition on EM grids. EM grids were reacted with anti-CAR monoclonal antibody, followed by a secondary antibody coupled to 20-nm colloidal gold particles, and examined under the EM. Under our experimental conditions, most anti-CAR gold grains were found to be associated with virus particles of CAR-pseudotyped BV^{CAR}, and exceptionally so in the background (Fig. 1b and c). Most baculovirions carried a single gold grain (Fig. 1d and e) and occasionally two, three, or more gold grains (Fig. 1f and g). With control parental BV virions incubated in parallel with anti-CAR and immunogold-labeled secondary antibody, we observed only background labeling (not shown).

As CAR-CAR interactions contribute to the intercellular tight junctions (24, 82), we expected to find BV^{CAR}-BV^{CAR} complexes under the EM. This was the case, and pairwise associations of BV^{CAR} virions lying side by side were observed (Fig. 2A, subpanels a to d), although at a low frequency (≤5% of total BV^{CAR} virions examined). Interestingly, after anti-

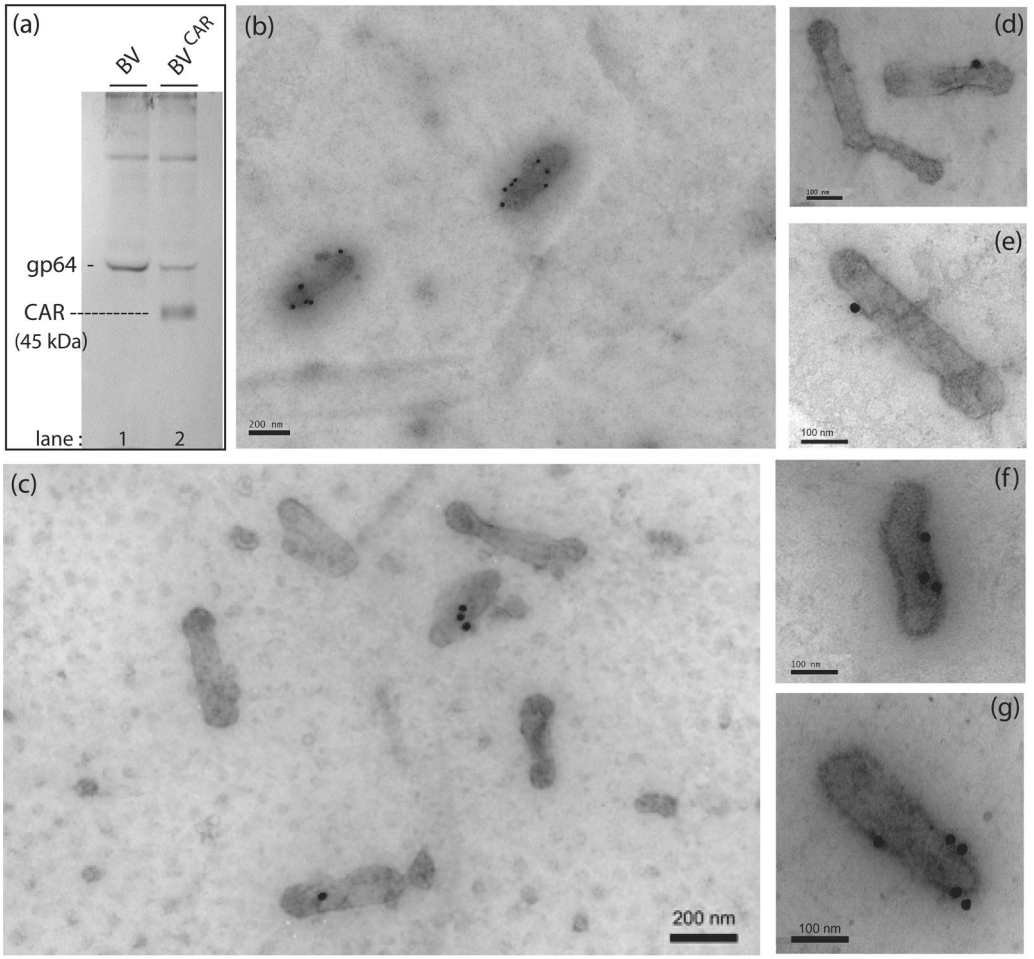

FIG. 1. Pseudotyping BV with human CAR glycoproteins. (a) Western blot analysis of control, parental (BV), and CAR-pseudotyped baculovirions (BV^{CAR}). BV (lane 1) and BV^{CAR} (lane 2) purified by ultracentrifugation were analyzed by SDS-PAGE and immunoblotting, using anti-gp64 and anti-CAR monoclonal antibodies and anti-mouse IgG conjugate. (b to g) Immuno-EM analysis. Virion samples deposited on grids were negatively stained with uranyl acetate and then reacted with monoclonal antibody against CAR, followed by anti-mouse antibody tagged with 20-nm colloidal gold. (b and c) General views of immunogold-stained BV^{CAR} preparations. Note the immunogold labeling associated with BV^{CAR} virions and the low level of background labeling. (d to g) Enlargement of anti-CAR gold-labeled BV^{CAR} virions. The number of grains associated per virion ranged from 0 (c and d) to 7 (b), with the highest frequency at 1, as shown in panels d and e.

CAR immunogold labeling of the BV^{CAR} samples adsorbed on grids, gold grains were often seen at the zone of contact between the two virions (Fig. 2A, subpanels a to d), suggesting that the BV^{CAR}-BV^{CAR} complexes occurred via true CAR-CAR interactions.

Efficiency of CAR pseudotyping of BV: quantitative aspects. The efficiency of pseudotyping of baculovirions by the foreign CAR glycoprotein was evaluated in comparison to the viral envelope glycoprotein gp64, a structural component of the virion called peplomer (70). Samples of BV^{CAR} virions were reacted on grids with a monoclonal antibody against gp64, followed by 20-nm colloidal gold-labeled anti-mouse IgG antibody, and examined under the EM. We found that most gold labeling localized near the head of the baculovirion (Fig. 2B), as expected from the gp64 topology (70).

The numbers of anti-gp64 and anti-CAR gold grains per virus particle were then counted in a population of 70 to 100 individual baculovirions. In our anti-gp64 labeling experiments, ca. 15% of baculovirions carried no grain, implying that this percentage represented the experimental threshold of detection for the baculoviral envelope glycoprotein gp64. For anti-CAR labeling, the number of unlabeled baculovirions was not significantly different and ranged from 16 to 23% (Fig. 3a). In both types of labeling, the most abundant population consisted of baculovirions carrying a single gold grain. Baculovirions with two, three, or more grains were found in both types of labeling, although at a significantly lower frequency (Fig. 3a; also Fig. 1 and 2). Taken together, these results indicated (i) that recombinant BV expressing CAR produced viral progeny pseudotyped by CAR glycoproteins and (ii) that the immunogold labeling (and hence the accessibility) of foreign CAR molecules on the BV^{CAR} envelope was almost as efficient as that of the structural gp64 glycoproteins.

Topology of CAR molecules at the surface of BV^{CAR} virions. To analyze the topology of gp64 and CAR molecules on the baculoviral envelope, we arbitrarily divided the baculovirions into 100 map units (mu) and measured the distance between the center of a 20-nm gold grain and the tip of the virus head.

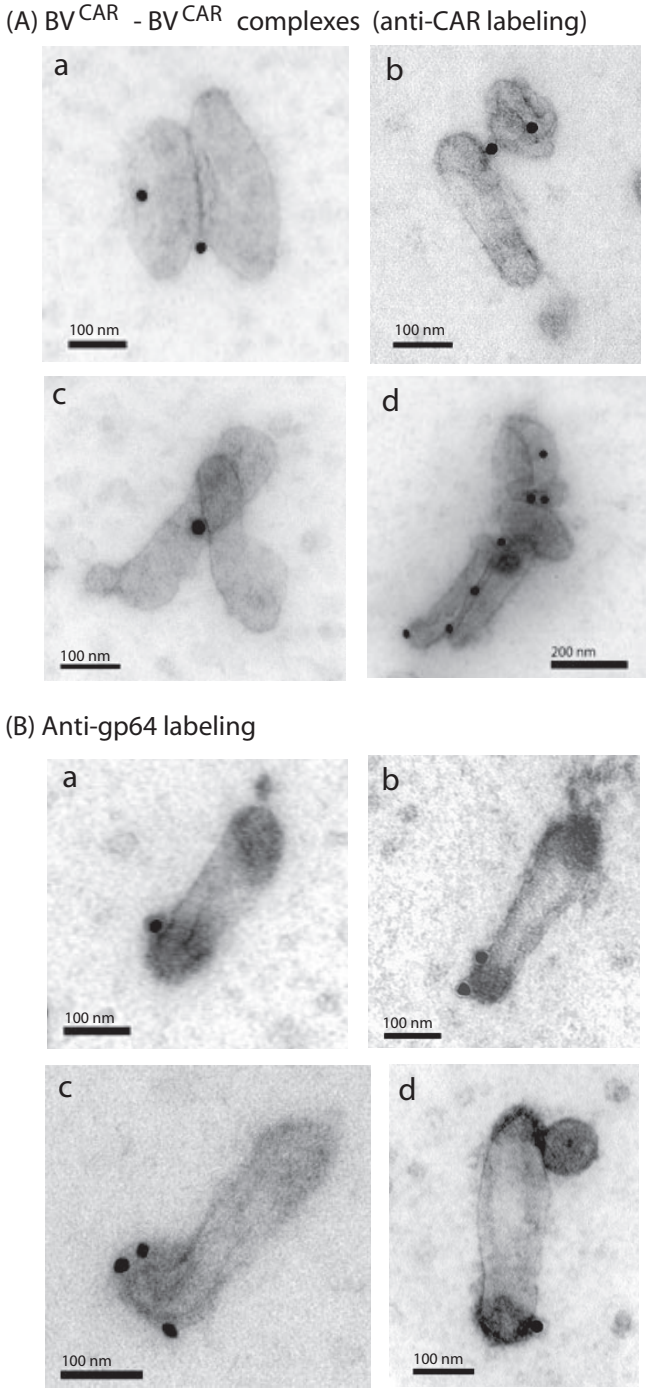

FIG. 2. EM and immuno-EM of BV^{CAR}. (A) Occurrence of BV^{CAR}-BV^{CAR} complexes. Samples of CAR-pseudotyped baculovirions (BV^{CAR}) were deposited on grids, negatively stained with uranyl acetate, and then reacted with monoclonal antibody against CAR, followed by anti-mouse antibody tagged with 20-nm colloidal gold, as in Fig. 1. Shown are spontaneously occurring pairwise (a to c) or multiple (d) associations of BV^{CAR} virions. (B) Anti-gp64 immunogold labeling of CAR-pseudotyped baculovirions. (a to c) BV^{CAR} virions deposited on grids were negatively stained with uranyl acetate and then reacted with monoclonal antibody against peplomer gp64, followed by anti-mouse antibody tagged with 20-nm colloidal gold grains. (d) Same reaction as in panels a to c performed on BV^{CAR}-Ad5GFP complexes deposited on grids. Note that gp64 and Ad5GFP virions are positioned at opposite poles of the baculovirion.

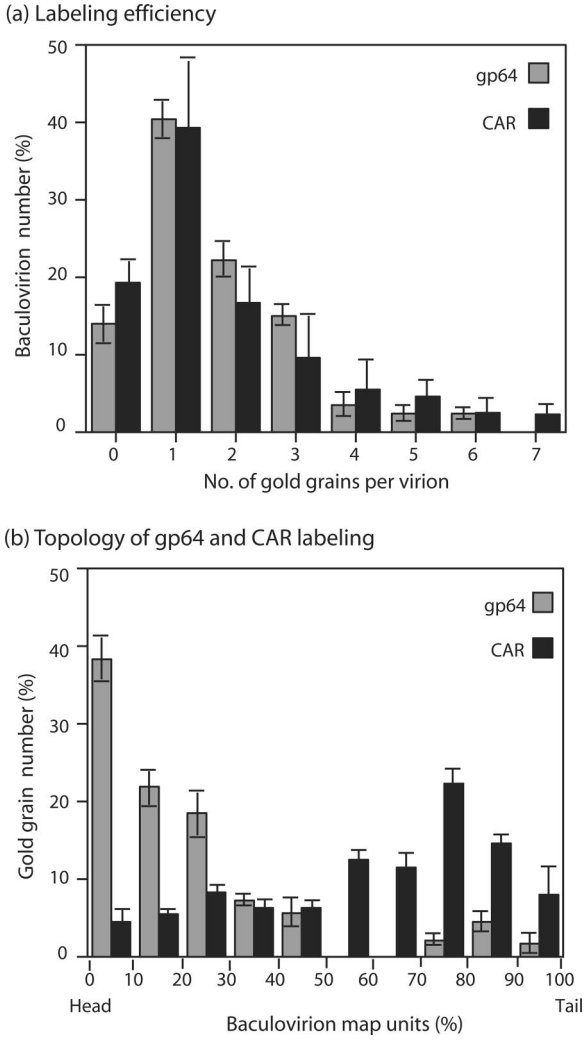

FIG. 3. Immunogold labeling of BV^{CAR}. (a) Comparison of the labeling efficiency of BV^{CAR} samples using anti-gp64 or anti-CAR monoclonal antibodies. The number of anti-gp64 and anti-CAR gold grains was counted per BV^{CAR} particle, in a population of 70 to 100 virions. (b) Topology of gp64 and CAR molecules on the baculoviral envelope, as determined by immunogold labeling. The position of gold grains on BV^{CAR} virions was determined by measuring the distance of the center of the gold grain to the tip of the virion head. Results were expressed as map units, defined as the percentage of the BV total length, which was assigned the 100% value. Shown are the means of three separate experiments ± SEMs.

In order to compensate for possible distortion and shrinking during the EM process, the results were expressed as the percentage of the full length of the virus (ca. 250 nm), with the virus head being taken as the origin (0%) and the end of the stem being assigned the 100% value. From our knowledge of BV structure (70), we could predict that most of the anti-gp64 gold grains would localize at or near the head of the baculovirions and not along their stem structure. Our EM observations were consistent with this prediction: nearly 40% of all anti-gp64 gold grains counted were found within 0 to 10 mu and 25% were found between 10 and 20 mu (Fig. 3b). Thus, almost two-thirds of the anti-gp64 gold grains localized within 0 to 50 nm. Considering that the approximate size of an IgG molecule

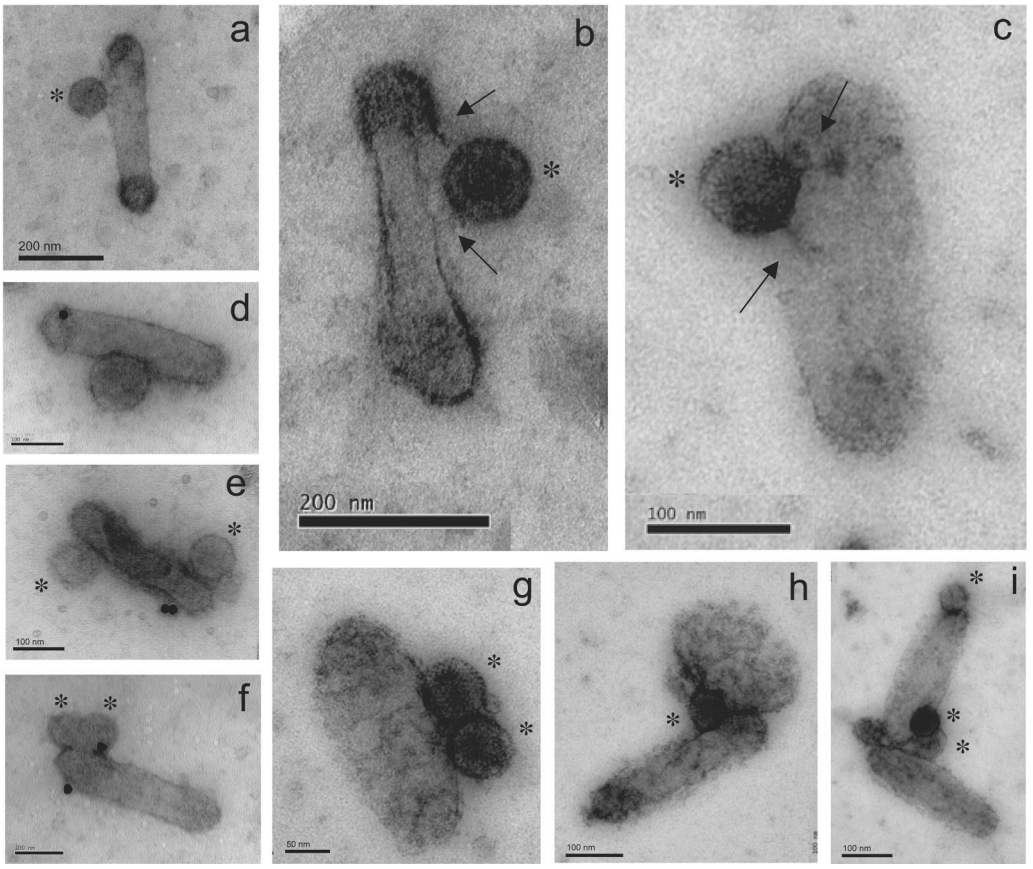

FIG. 4. EM and immuno-EM of BV^{CAR}-Ad5GFP complexes. BV^{CAR}-Ad5GFP complexes deposited on grids were negatively stained with uranyl acetate and examined under the EM (a to c and g to i) or further incubated with anti-CAR monoclonal antibody and 20-nm colloidal gold-tagged anti-mouse antibody (d to f), in order to test the anti-CAR reactivity of the BV^{CAR}-Ad5GFP complex. Ad5GFP virions are marked with asterisks. Panels a to d show BV^{CAR} virions associated with a single particle of Ad5GFP, whereas panels e to g show BV^{CAR} virions associated with two Ad5GFP particles. Panels b and c are enlargements of BV^{CAR}-Ad5GFP complexes showing filamentous structures connecting adenovirions to the baculoviral envelope (arrows). Note that CAR molecules were not all occupied by Ad5GFP virions, since anti-CAR antibodies still reacted with the complexes (d to f). Panels h and i show Ad5GFP virions bridging two BV^{CAR} virions.

is about 15 nm under the EM, the BV-associated primary and secondary antibodies accounted for 30 nm in length and the colloidal gold accounted for an extra 20 nm. The immuno-EM pattern of gp64 labeling was therefore compatible with the localization of the gp64 at the baculoviral pole. In contrast to gp64, the anti-CAR labeling showed a polydisperse pattern: anti-CAR gold grains were found all along the stem of the BV^{CAR} virions, with some preferential sites between 70 and 90 mu (Fig. 3b; also Fig. 1d to g). This suggested that the CAR molecules were excluded from the polar region of the baculoviral envelope in which the gp64 peplomers were inserted. This was confirmed by EM analyses of BV^{CAR}-Ad5GFP complexes, as shown (Fig. 4).

Functionality of human CAR attachment molecules on the baculoviral envelope: occurrence of BV^{CAR}-Ad5GFP complexes. We next determined whether CAR glycoproteins present at the surface of the baculovirion were functional as attachment molecules for Ad5. BV^{CAR} virions were mixed with the same number of Ad5GFP vector particles, incubated for 1 h at 37°C, and examined under the EM after negative staining. Different types of BV^{CAR}-Ad5GFP association were observed, but the most frequently seen consisted of binary complexes, or virus duos, composed of one baculovirion bound to one adenovirion (Fig. 4a to d). Ternary complexes, or virus trios, formed of one BV^{CAR} carrying two Ad5GFP were more rarely observed (Fig. 4e to g). Modifications of the particle ratio between BV^{CAR} and Ad5GFP in the incubation mixture did not change significantly this EM pattern (not shown).

In the majority of the BV^{CAR}-Ad5GFP binary complexes, the Ad particles were found to bind to the stem of BV^{CAR}, an observation consistent with the localization of CAR molecules on the BV^{CAR} envelope, as determined by our anti-CAR immunogold labeling (Fig. 3b). Since an adenovirion carries 12 fiber projections and is therefore multivalent in terms of attachment, we expected that Ad5GFP could bridge two or more BV^{CAR} particles. Such higher-order complexes were observed under the EM, although on rare occasions: they mainly consisted of ternary complexes formed of one Ad5GFP bound to two BV^{CAR} particles (Fig. 4h and i).

Examination of BV^{CAR}-Ad5GFP complexes under the EM at high resolution revealed that some adenovirions were linked to their BV carriers via filamentous structures which resembled the adenoviral fiber. In some cases, two filaments could be distinguished (Fig. 4b and c, arrows). This suggested that the

binding of Ad5GFP to CAR molecules could occur via more than one valence.

This observation raised the question of the degree of occupancy and/or accessibility of CAR molecules inserted in the baculoviral envelope. To address this issue, BV^{CAR}-Ad5GFP complexes were reacted on grids with anti-CAR antibody followed by secondary 20-nm gold-tagged antibody, as described above. Many individual BV^{CAR} particles which were associated with one or two Ad5GFP particles were still labeled by anti-CAR and carried one (Fig. 4d) or several (Fig. 4e and f) gold grains. This indicated that when BV^{CAR}-Ad5GFP complexes were formed in a binding reaction involving equal numbers of the two viruses, several CAR molecules present at the BV^{CAR} surface were still unoccupied and available for anti-CAR antibody binding or CAR-CAR interaction. This was also suggested by the anti-CAR labeling of BV^{CAR}-BV^{CAR} complexes shown in Fig. 2A. Taken together, these results indicated that CAR functioned as a bona fide Ad5 attachment molecule at the surface of the baculovirions.

Transduction of CAR-negative CHO cells by BV^{CAR}-Ad5GFP complex. (i) Transduction efficiency. The functionality of our BV^{CAR}-Ad5GFP complex and the capacity of BV^{CAR} to mediate Ad5 gene delivery by overcoming the lack of CAR at the cell surface were first assessed on CHO cells, which are CAR negative and poorly permissive to Ad5 (3). The transduction level obtained with a BV^{CAR}-Ad5GFP complex generated with a ratio of Ad5GFP to BV^{CAR} vp (physical particles) of 1 to 10 in the mix was greatly enhanced, compared to Ad5GFP alone at a similar MOI of Ad5GFP vector (Fig. 5A, subpanels a and c). As quantified by flow cytometry, 65 to 70% of CHO cells were transduced by the BV^{CAR}-Ad5GFP complex at an MOI range of 100 to 500 in terms of Ad5GFP vp/cell, compared to 10 to 15% in control samples transduced by Ad5GFP alone at the same MOI (Fig. 5B, subpanel a).

(ii) Contribution of BV^{CAR} to the augmentation of Ad5-mediated transduction efficiency. The role of BV^{CAR} in the transduction enhancement by the complex was evaluated using BV^{CAR}GFP alone. BV^{CAR}GFP was a recombinant AcMNPV expressing the GFP gene under the control of the CMV promoter (the same promoter as that in Ad5GFP) and was pseudotyped with CAR by coinfection of Sf9 cells with BV^{CAR}. The level of CHO cell transduction obtained with BV^{CAR}GFP (Fig. 5A, subpanel b) was lower than that with the BV^{CAR}-Ad5GFP complex but higher than that with Ad5GFP at the same MOI (Fig. 5A, subpanels c and a, respectively). This suggested that both viruses contributed to the enhancing effect on transduction by the virus duo but that BV^{CAR} contributed to a higher level than did Ad5GFP.

(iii) Specificity of transduction by BV^{CAR}-Ad5GFP complex. CHO-CAR is a CHO-derived cell line which constitutively expresses CAR and is fully susceptible to Ad5 infection (3). CHO-CAR cells were infected with BV^{CAR}-Ad5GFP, at a constant MOI of BV^{CAR} and various MOIs of Ad5GFP, or with Ad5GFP alone at the same MOI as that in the complex. At a low MOI (less than 50 vp/cell, corresponding to 2 to 5 PFU/cell), CHO-CAR cells were transduced with a slightly higher efficiency by BV^{CAR}-Ad5GFP than by Ad5GFP alone (1.5- to 2-fold; Fig. 5B, subpanel b), but this effect was no longer observed at a higher MOI (100 to 500 vp/cell; Fig. 5B, subpanel b). The absence of enhanced transduction of Ad5-permissive cells by the BV^{CAR}-Ad5GFP complex suggested that this effect was specific in nature.

(iv) Role of CAR glycoproteins in BV^{CAR}-mediated cell transduction. The AcMNPV envelope glycoprotein gp64 represents the major cell attachment component of this virus (59). Gp64 binds to insect cell plasma membrane receptors (70), as well as to a large repertoire of mammalian cell surface glycoproteins (31, 32, 41). In order to determine the respective roles of baculoviral gp64 and extrinsic CAR glycoprotein in the efficiency of cell transduction, CHO and CHO-CAR cells were incubated with the CAR-pseudotyped vector BV^{CAR}GFP at different MOIs. CHO-CAR cells were found to be significantly more permissive to BV^{CAR}GFP than were CHO cells (two- to threefold; Fig. 5C). This suggested that BV^{CAR}GFP could use different pathways to attach to and enter CHO cells, e.g., one involving gp64 and its cellular ligand(s) and the other mediated by interaction between BV-displayed CAR molecules and cell plasma membrane-exposed CAR. This was reminiscent of the CAR-CAR interaction suggested by the EM observation of dimers of CAR-pseudotyped baculovirions (Fig. 2A).

Transduction of CAR-negative human cells by BV^{CAR}-Ad5GFP complex. (i) Nontumor cell line. Human glandular tracheal cells (MM39) fail to express CAR and are poorly permissive to Ad5 (14, 15, 17). As was observed with CHO cells, a net augmentation of the transduction efficiency was obtained when MM39 cells were incubated with BV^{CAR}-Ad5GFP, compared to control MM39 samples transduced with a single vector at the same MOI, Ad5GFP or BV^{CAR}GFP (Fig. 6A).

(ii) Cancer cell lines. Gene transduction mediated by BV^{CAR}-Ad5GFP complexes was also evaluated on rhabdomyosarcoma cells (RD), ovarian carcinoma cells (SKOV3), and breast carcinoma cells (SKBR3), three human cancer cell lines which were poorly transduced by Ad5 (20). The efficacy of BV^{CAR}-Ad5GFP transduction was significantly higher than that of transduction with Ad5GFP alone for the three types of cancer cells (Fig. 6B). For RD cells, the percentage of transduced cells improved by almost 1 order of magnitude, from 5% with Ad5GFP to 45% with BV^{CAR}-Ad5GFP, and for SKOV3 cells, the augmentation was seven- to eightfold higher, from 2.5% (with Ad5GFP) to 21% (with BV^{CAR}-Ad5GFP). However, in the case of SKBR3 cells, which were slightly permissive to Ad5, the increase in transduction was only two- to threefold, from 12% (Ad5GFP) to 35% (BV^{CAR}-Ad5GFP). As for CHO and MM39 cells, the levels of transduction of RD and SKBR3 cells by the control vector BV^{CAR}GFP alone was intermediate between those of Ad5GFP and BV^{CAR}-Ad5GFP. Interestingly, the level of SKOV3 transduction was almost equivalent using BV^{CAR}-Ad5GFP and using BV^{CAR}GFP (Fig. 6B), confirming that the contribution of BV^{CAR} to the transduction enhancement by the BV^{CAR}-Ad5GFP complex was greater than that of Ad5GFP.

Transduction of human primary cells by BV^{CAR}- Ad5GFP complex. Several types of human primary cells have been reported to be refractory to or poorly transduced by Ad5 vectors, e.g., dermal fibroblasts and synoviocytes (76). These cells were transduced with aliquots of virus inoculum containing increasing MOIs of Ad5GFP mixed with a constant BV^{CAR} input (500 vp/cell) and analyzed by fluorescence microscopy and flow cytometry. For dermal fibroblasts, a progressive increase in transduction was observed with increasing MOIs of Ad5GFP, and the maximum transduction efficiency (82% GFP-positive

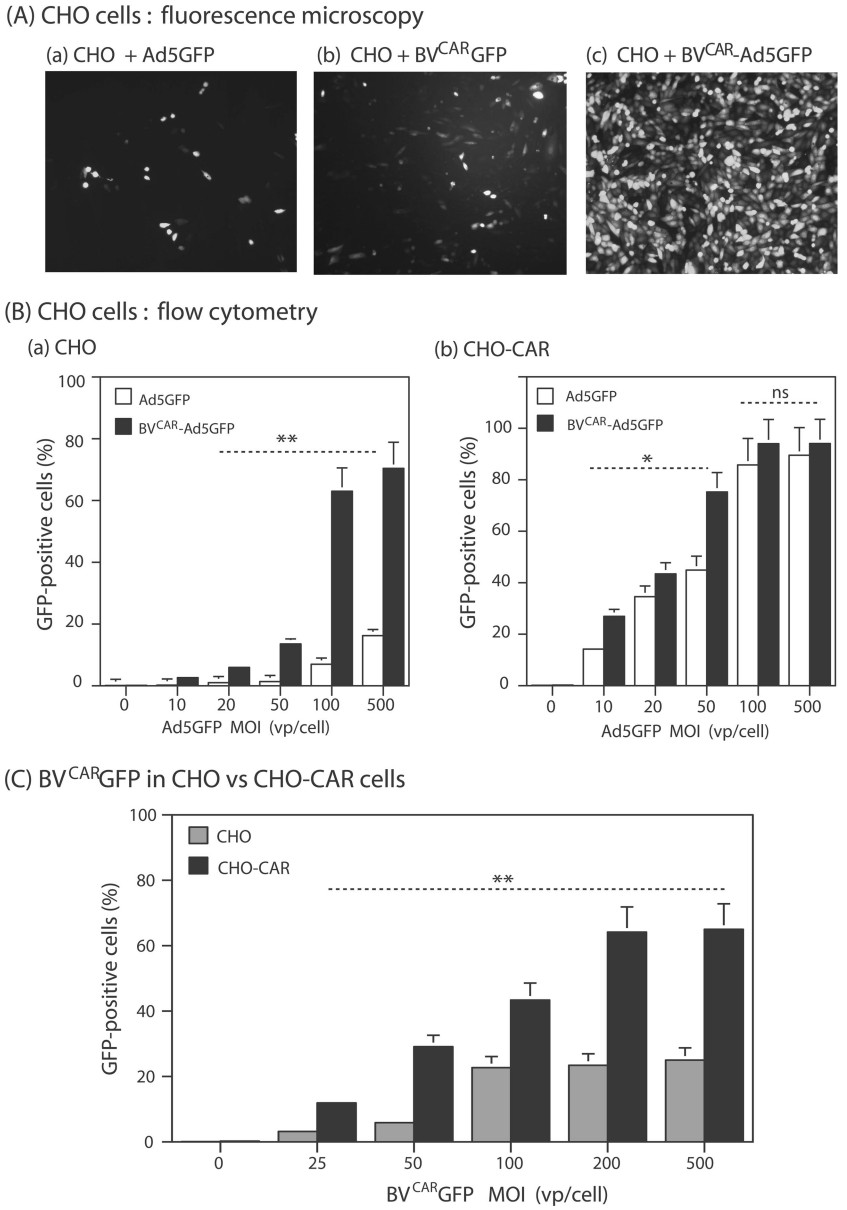

FIG. 5. Transduction of CAR-negative (CHO) or CAR-positive (CHO-CAR) cells by BV^{CAR}-Ad5GFP complex. (A) Fluorescent microscopy. CHO cells were transduced by Ad5GFP alone (MOI of 100 vp/cell) (a), BV^{CAR}GFP alone (1,000 vp/cell) (b), or BV^{CAR}-Ad5GFP complex (Ad5GFP MOI of 100 vp/cell; Ad5GFP/BV^{CAR} vp ratio of 1:10) (c). (B) Flow cytometry. Bar graph representation of the efficiency of transduction of CHO (a) or CHO-CAR (b) by Ad5GFP alone (open bars) or BV^{CAR}-Ad5GFP complex (solid bars). Complexes were generated by mixing a constant amount of BV^{CAR} (corresponding to 500 vp/cell) with increasing amounts of Ad5GFP, as indicated on the *x* axis. (C) Transduction efficiency of CHO cells by control vector BV^{CAR}GFP. Flow cytometry analysis of CHO cells (gray bars) or CHO-CAR cells (black bars) transduced by BV^{CAR}GFP alone at increasing MOIs, as indicated on the *x* axis. Results, expressed as the percentages of GFP-positive cells, represent the means of three separate experiments ± SEMs. *, $P < 0.05$; **, $P < 0.01$; ns, no significant difference.

cells) was reached at an Ad5GFP MOI of 20 vp/cell (Fig. 7a). Transduction of synoviocytes using BV^{CAR}-Ad5GFP complex was analyzed using the same range of viral complex inputs. Synoviocytes were moderately permissive to Ad5, and only 20% of cells were transduced at an Ad5GFP MOI of 20 vp/cell. However, a transduction of 80% of cells was obtained using the BV^{CAR}-Ad5GFP complex at the Ad5GFP dose of 20 vp/cell (Fig. 7b).

The efficiency of the BV^{CAR}-Ad5GFP complexes was also tested on human MSCs. MSCs were transduced to about 25 to 28% with BV^{CAR}-Ad5GFP, versus 2% with Ad5GFP alone at an MOI of 20, i.e., a 10-fold increase (Fig. 7c). In the case of immature monocyte-derived DCs, there was a moderate increase in transduction with BV^{CAR}-Ad5GFP (twofold), and the number of GFP-positive DCs plateaued at around 12 to 15% at the relatively high Ad5GFP MOI of 500 vp/cell (Fig. 7d). For PBMCs, the transduction levels were low, but the increase was significant, from 0.1% with Ad5GFP alone to 2%

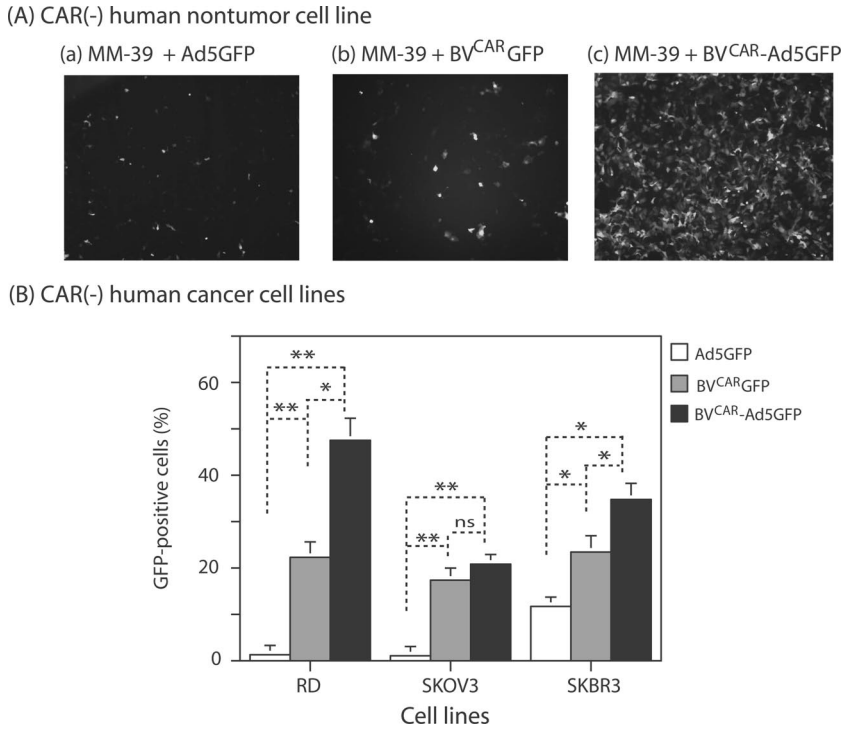

FIG. 6. Transduction of CAR-negative human cell lines by BV^{CAR}-Ad5GFP complex. (A) Nontumor cells. Fluorescent microscopy of MM39 cells transduced by Ad5GFP alone (MOI of 20 vp/cell) (a), BV^{CAR}GFP alone (500 vp/cell) (b), or BV^{CAR}-Ad5GFP complex (Ad5GFP MOI of 20 vp/cell; Ad5GFP/BV^{CAR} vp ratio of 1:25) (c). (B) Tumor cells. Flow cytometry analysis of human cancer cell lines RD, SKOV3, and SKBR3 transduced by Ad5GFP alone (20 vp/cell), BV^{CAR}GFP alone (500 vp/cell), or BV^{CAR}-Ad5GFP complex (Ad5GFP MOI of 20 vp/cell; Ad5GFP/BV^{CAR} vp ratio of 1:25). Results, expressed as the percentages of GFP-positive cells, represent the means of three separate experiments ± SEMs. *, $P < 0.05$; **, $P < 0.01$; ns, no significant difference.

with BV^{CAR}-Ad5GFP at an Ad5GFP MOI of 1,000 vp/cell (Fig. 7e). As for CHO, RD, and SKBR3 cells, the levels of transduction of the primary cells treated with control vector BV^{CAR}GFP was intermediate between those of Ad5GFP and BV^{CAR}-Ad5GFP (Fig. 7).

Requirements for BV^{CAR}- Ad5GFP complex formation and cell transduction enhancement. (i) Transduction efficiency versus ratio of BV^{CAR} to Ad5GFP particles. In order to determine the optimal conditions for cell transduction by the biviral complex, we prepared a range of BV^{CAR}-Ad5GFP mixtures differing in their ratios of BV^{CAR} to Ad5GFP vp and assayed their gene transfer efficiency on two types of primary cells, dermal fibroblasts and synoviocytes. In one set of transduction experiments, the number of BV^{CAR} vector particles was kept constant (500 vp/cell) and Ad5GFP MOI varied from 0.1 to 20 vp/cell. For both cell types, the level of transduction increased in an Ad5GFP dose-dependent manner and 80 to 85% of cells were found to be GFP positive at 20 vp/cell (Fig. 8a). In another set of experiments, Ad5GFP MOI was kept constant (20 vp/cell) whereas BV^{CAR} particles varied from 0 to 1,000 vp/cell (Fig. 8b). A plateau of maximum cell transduction (80 to 85% GFP-positive cells) was obtained for both cell types at a ratio of 20 Ad5GFP to 500 BV^{CAR} particles (Fig. 8b). Increasing the number of BV^{CAR} particles over this value did not augment the transduction efficiency (Fig. 8b).

A wider range of Ad5GFP to BV^{CAR} vp ratios was then tested, and the transduction efficiency was represented as a function of the vp ratio values (Fig. 8c). The bar graph representation followed the Gaussian mode, with the highest transduction efficiency obtained at a ratio of 100 BV^{CAR} to three Ad5GFP particles. We interpreted this value in terms of cell transduction as the result of several parameters influencing the cell transduction. These included (i) the occurrence of a certain number of CAR-negative BVs in the population of virus carrier, as shown above; (ii) the dissociation constant of the equilibrium reaction between free and BV^{CAR}-bound Ad5GFP in the mixture, which has not been experimentally determined for Ad5 virion and pseudotyped BV^{CAR}; and (iii) the cellular response to this viral duo. Unless otherwise stated, we generated BV^{CAR}-Ad5GFP complexes using vp ratios ranging from 20 BV^{CAR}:1 Ad to 30 BV^{CAR}:1 Ad.

(ii) Knob dependence of the Ad5GFP-BV^{CAR} liaison. In order to verify that the Ad5 virions present within the BV^{CAR}-Ad5GFP complexes bound to BV^{CAR} via their fiber knob domain, we transduced dermal fibroblasts with a mixture of BV^{CAR} (at a constant MOI of 500 vp/cell) and Ad5GFP-R7ΔKnob (at increasing MOIs). Ad5GFP-R7ΔKnob carried knob-deleted (ΔKnob) short-shafted fibers of seven repeats (R7) and lacked its CAR-binding domains (20, 28, 50, 51). No detectable enhancement of Ad5GFP-R7ΔKnob-mediated transduction was observed in the presence of BV^{CAR}, compared to Ad5GFP-R7ΔKnob alone, implying that the integrity of the knob domain was indispensable for the positive effect of BV^{CAR} on Ad5 transduction (Fig. 9a).

(iii) Requirement for CAR on the envelope of BV^{CAR}. The enhancement of Ad5GFP-mediated cell transduction in the

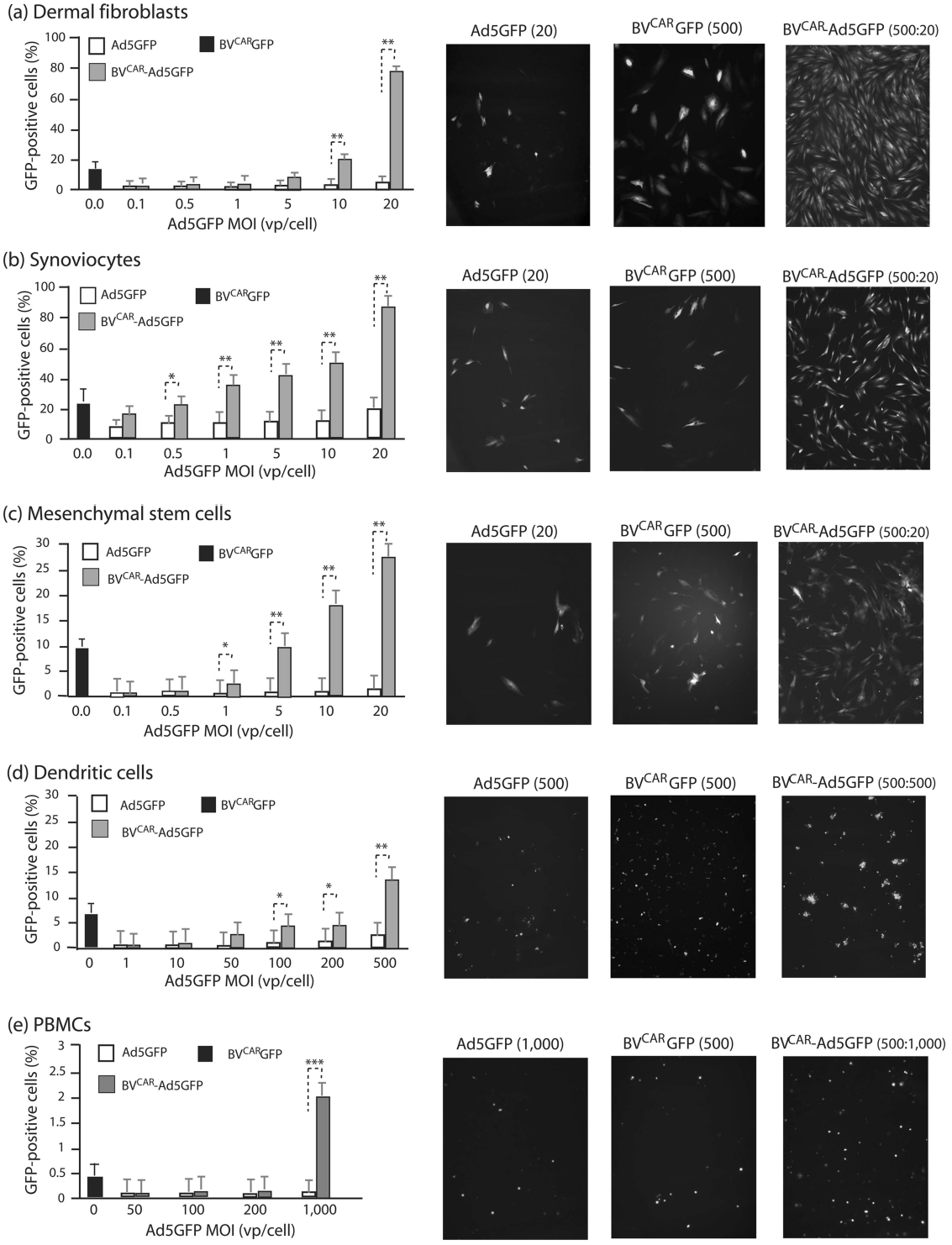

FIG. 7. Transduction of CAR-negative human primary cells by BV^{CAR}-Ad5GFP complex. Graphs on left show flow cytometry results. Bar graph representation of the efficiency of gene transfer mediated by Ad5GFP alone versus BV^{CAR}-Ad5GFP complex in different human primary cells, as indicated above each panel. Cells were transduced by Ad5GFP alone at increasing MOIs or by BV^{CAR}-Ad5GFP complexes at a constant MOI of BV^{CAR} (500 vp/cell) and increasing MOIs of Ad5GFP, as indicated on the *x* axis. Results, expressed as the percentages of GFP-positive cells, represent the means of three separate experiments ± SEMs. The black bars on the far left of the graphs represent the values obtained with the control baculoviral vector BV^{CAR}GFP alone, at an MOI of 500 vp/cell. The right panels show fluorescent microscopy results. Shown are cell samples transduced at the maximal infectivity of each separate vector or biviral complex, as indicated above each panel. Cells were transduced by Ad5GFP alone (left), BV^{CAR}GFP alone (middle), or BV^{CAR}-Ad5GFP complex (right). *, $P < 0.05$; **, $P < 0.01$; ***, $P < 0.005$.

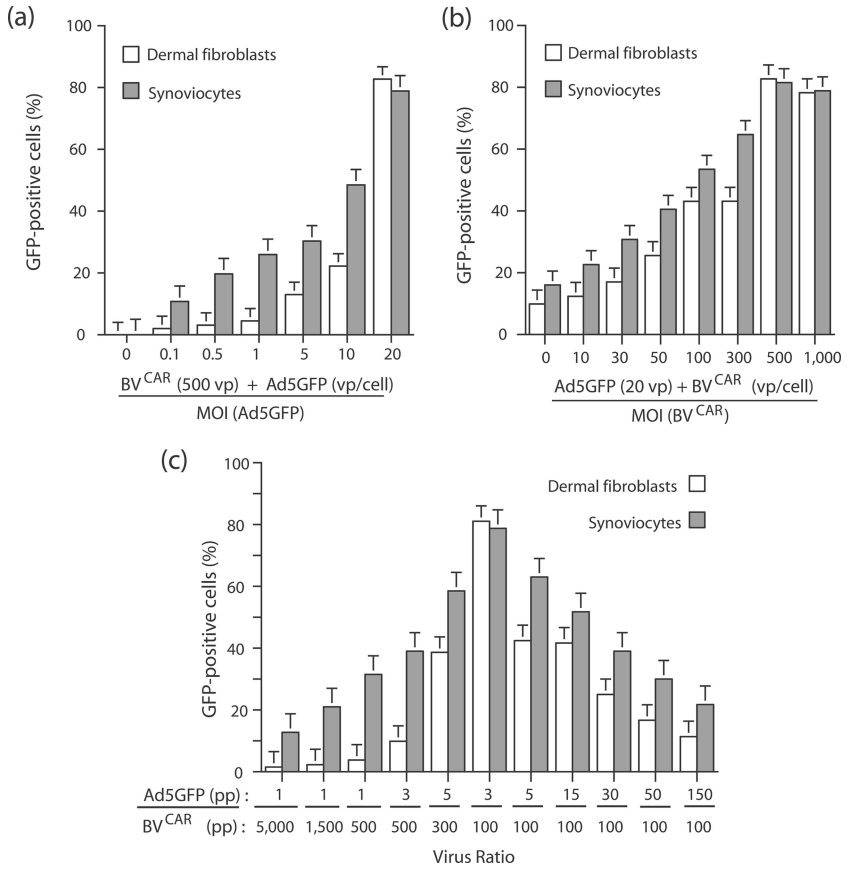

FIG. 8. Influence of BV^{CAR}-to-Ad5GFP ratios on BV^{CAR}-Ad5GFP-mediated transduction of human primary cells. (a) Dermal fibroblasts and synoviocytes were transduced by BV^{CAR}-Ad5GFP complex generated using a constant MOI of BV^{CAR} (500 vp/cell) and various MOIs of Ad5GFP, as indicated on the *x* axis. (b) Cells were transduced by BV^{CAR}-Ad5GFP complex generated using a constant MOI of Ad5GFP (20 vp/cell) and various MOIs of BV^{CAR}, as indicated on the *x* axis. (c) Cell transduction efficiency by BV^{CAR}-Ad5GFP complex was evaluated using a wide range of BV^{CAR}-to-Ad5GFP ratios. The transduction efficiency was expressed as the percentage of GFP-positive cells, assayed by flow cytometry (means of three separate experiments ± SEMs).

presence of BV^{CAR} might be due to a certain degree of nonspecific cellular engulfment of Ad5 vector in the presence of baculovirions and not to the formation of BV^{CAR}-Ad5GFP complex via specific CAR-fiber knob interaction. To address this issue, we mixed Ad5GFP at a constant MOI (10 vp/cell) with nonpseudotyped, parental vector BV at various doses (0, 250, and 500 vp/cell) and analyzed the transduction level of synoviocytes and dermal fibroblasts using the mixture of unbound viruses, in comparison with the transduction mediated by BV^{CAR}-Ad5GFP complexes generated with the same virus ratios. No significant effect on the level of cell transduction was observed with the mixtures of unbound viruses, compared to the corresponding BV^{CAR}-Ad5GFP complexes (Fig. 9b). This indicated that the enhancing effect on cell transduction by the complex depended on the presence of CAR molecules at the surface of the baculovirions and on CAR-mediated interaction with Ad5GFP.

(iv) Blockage of BV^{CAR}-Ad5GFP-mediated cell transduction by anti-CAR antibody. To further demonstrate the role of CAR glycoprotein in bridging Ad5GFP to BV^{CAR} in the dual virus mixture, we analyzed the effect of an anti-CAR monoclonal antibody on dermal fibroblast transduction. Anti-CAR antibody was added at different dilutions during (Fig. 9c) or after (Fig. 9d) the step of virus mixing, when CAR-fiber bonds had already formed. When anti-CAR antibody was added simultaneously to the viral mixture, inhibition of gene transfer was observed in a dose-response manner, and the basal level of transduction was reached in the presence of undiluted antibody sample (Fig. 9c). In contrast, when anti-CAR antibody was added after the mixing, no effect in Ad5 gene transfer was detected (Fig. 9d). These results confirmed the role of CAR in the generation of BV^{CAR}-Ad5GFP complex and its requirement for the cell transduction enhancement.

Mechanism of cellular uptake of BV^{CAR}-Ad5GFP complex. (i) Kinetics of cell binding and uptake of BV^{CAR}-Ad5GFP. There are several parameters, in addition to baculoviral tropism, that might lead to the superior transduction of CAR-negative cells by the dual vector BV^{CAR}-Ad5GFP. In order to investigate the possible kinetic benefits of this complex, CHO cells were incubated with Ad5GFP alone or BV^{CAR}-Ad5GFP complex at the same MOI in terms of Ad5GFP vector, and the number of cell-associated virions was determined at 10-min intervals during the first hour of virus-cell attachment, using real-time quantitative PCR. The number of Ad5 genome copies recovered per cell was found to be twofold higher for BV^{CAR}-Ad5GFP at all time points than for control Ad5GFP.

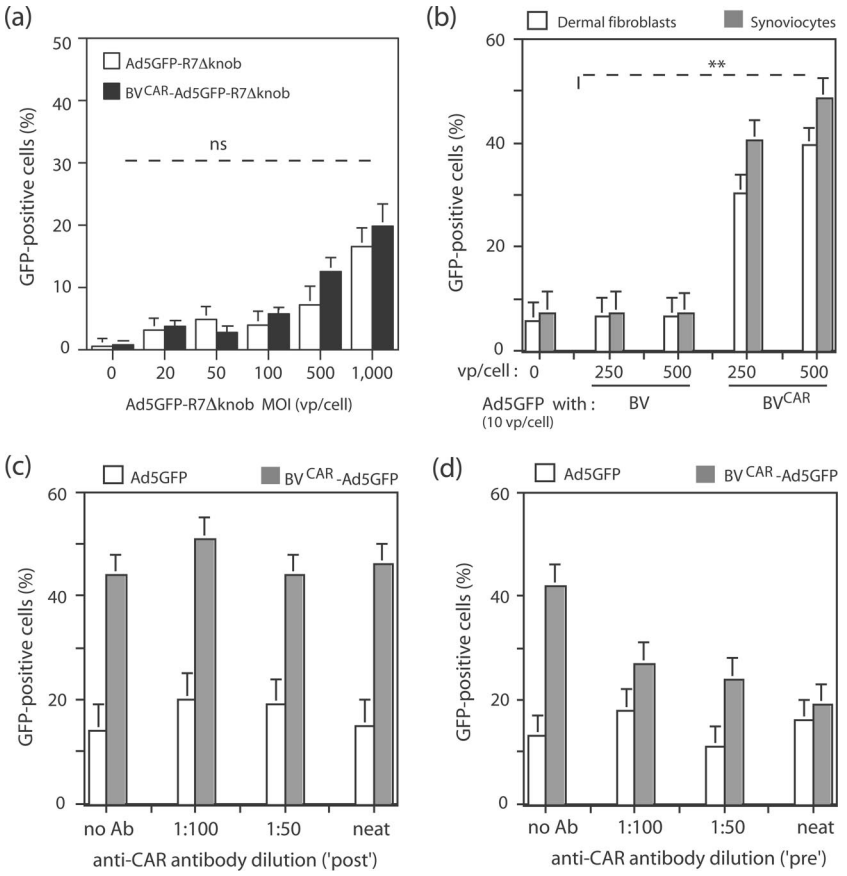

FIG. 9. Role of CAR and fiber knob in BV^{CAR}-Ad5GFP-mediated cell transduction. (a) Requirement for the fiber knob domain in Ad5GFP vector. Human dermal fibroblasts were transduced by Ad5GFP-R7ΔKnob alone at increasing MOIs or a mixture of BV^{CAR} at a constant MOI (500 vp/cell) and Ad5GFP-R7ΔKnob at increasing MOIs, as indicated on the *x* axis. (b) Requirement for CAR glycoprotein on the baculoviral membrane. Human dermal fibroblasts and synoviocytes were transduced by a mixture of Ad5GFP and BV^{CAR} or a mixture of Ad5GFP and nonpseudotyped BV (parental AcMNPV empty vector) at a constant MOI of Ad5GFP (10 vp/cell) and various BV or BV^{CAR} inputs at MOIs of 0, 250, and 500 vp/cell. (c and d) Requirement for CAR-fiber interaction. Human dermal fibroblasts were transduced by a mixture of BV^{CAR} (MOI of 250 vp/cell) and Ad5GFP (20 vp/cell), containing anti-CAR monoclonal antibody added at different dilutions. In panel c, anti-CAR antibody was added after complex formation, by premixing the two viruses followed by incubation for 1 h at 37°C ("post"). In panel d, anti-CAR antibody was added simultaneously with both viruses before complex formation ("pre"). Virus samples and antibody were further incubated for 1 h at 37°C. Controls consisted of Ad5GFP samples at the same MOI incubated with the same antibody dilutions. Results were expressed as the percentages of GFP-positive cells, assayed by flow cytometry (means of three separate experiments ± SEMs). **, $P < 0.01$; ns, no significant difference.

In addition, the slope of the curves of cell-bound viruses versus time indicated that the cellular uptake of Ad5GFP complexed with BV^{CAR} occurred at a significantly higher rate than that of Ad5GFP alone (twofold; Fig. 10a). In contrast, the cell binding kinetics of BV^{CAR} and the number of cell-associated baculoviral genome copies did not change significantly when BV^{CAR} was alone or in complex with Ad5 (Fig. 10b). These data suggested that the presence of BV^{CAR} in the complex provided significant kinetic benefits to Ad5GFP and not only an advantage in terms of cell tropism. Interestingly, the ratio of viral genomes recovered from BV^{CAR}-Ad5GFP-infected cells at 30 to 50 min p.i. (two Ad5GFP to 50 to 60 BV^{CAR}) corresponded to the ratio required for optimal cell transduction (Fig. 8c).

(ii) Role of baculoviral glycoprotein gp64. We next addressed the question of whether the envelope glycoprotein gp64 of BV^{CAR} was involved in the cell attachment and uptake of the BV^{CAR}-Ad5GFP complex, using dermal fibroblasts as the cellular target. We found that the BV^{CAR}-Ad5GFP-mediated gene transfer was inhibited in the presence of anti-gp64 monoclonal antibody in a dose-dependent manner, suggesting that gp64 was the major attachment protein of the complex (Fig. 10c). However, cell transduction was not totally inhibited, and the inhibitory effect plateaued at a residual value equivalent to twofold the basal level of transduction observed with Ad5GFP alone (Fig. 10c). This suggested that a baculoviral envelope glycoprotein(s) other than gp64 (e.g., CAR) might play a role in the cell attachment of BV^{CAR}-Ad5GFP and/or that the residual transduction was due to an alternative cell entry pathway, e.g., via macropinocytosis.

(iii) Influence of Ad5 virions on BV^{CAR}-Ad5GFP-mediated cell transduction: endosomal escape and cell entry. It is known that Ad5 is very efficient in endosomal escape, and this represents one of its advantages as a gene vector (14, 26, 65). In order to determine whether the adenoviral moiety of the BV^{CAR}-Ad5GFP complex was beneficial to the internalization of baculovirions, we used GFP-expressing BV vectors with or

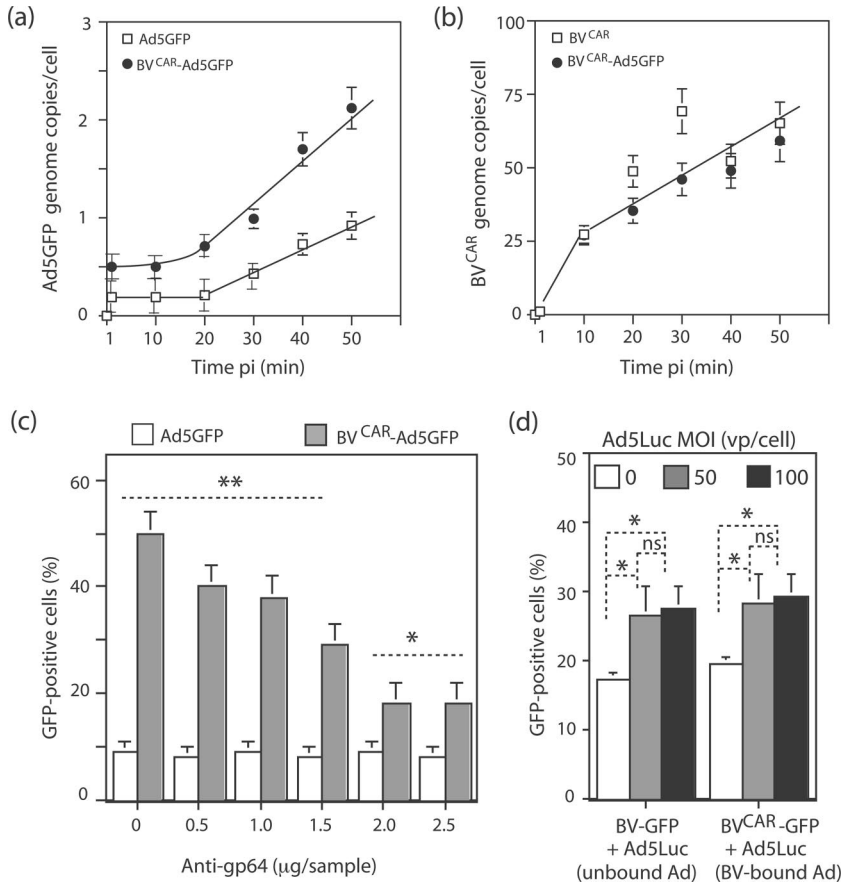

FIG. 10. Mechanism of cellular uptake of the BV^{CAR}-Ad5GFP complex. (a and b) Cell binding kinetics. Ad5GFP alone (open symbols), BV^{CAR} alone (open symbols), or BV^{CAR}-Ad5GFP complex (filled symbols) was incubated with CHO cells at 37°C for 50 min, and cell samples were withdrawn every 10 min p.i. After washing, cell-associated virions were assayed in cell lysates using real-time quantitative PCR. Results were expressed as the numbers of adenoviral and baculoviral genomes recovered per cell, using the beta-actin gene as an internal control. (a) Ad5GFP genomes: Ad5GFP alone ($y = 0.24x$, $R^2 = 0.993$) and BV^{CAR}-Ad5GFP complex ($y = 0.49x$, $R^2 = 0.977$). (b) BV^{CAR} genomes ($y = 10.5x$, $R^2 = 0.91$). (c) Role of baculoviral gp64. BV^{CAR}-Ad5GFP complex, at the BV^{CAR}/Ad5GFP MOI ratio of 500:20 vp/cell, was preincubated for 1 h at 37°C with different dilutions of anti-gp64 monoclonal antibody and added to monolayers of human dermal fibroblasts. (d) Role of the Ad5GFP moiety in cell internalization of BV^{CAR}-Ad5GFP complex. Human MSCs were transduced with a mixture of nonpseudotyped, GFP-expressing baculoviral vector BV-GFP and Ad5Luc (Ad5-unbound BV-GFP; leftmost bars) or a mixture of CAR-pseudotyped, GFP-expressing baculoviral vector BV^{CAR}GFP with Ad5Luc (Ad5-bound BV-GFP; rightmost bars). BV-GFP and BV^{CAR}GFP were used at constant MOIs each (MOI of 500), and Ad5Luc was used at different MOIs (0, 50, and 100). The transduction efficiency was expressed as the percentage of GFP-positive cells, assayed by flow cytometry (means of three separate experiments ± SEMs). *, $P < 0.05$; **, $P < 0.01$; ns, no significant difference.

without CAR pseudotyping, BV^{CAR}GFP and BV-GFP, respectively. BV^{CAR}GFP vector was incubated with Ad5Luc, an Ad5 vector expressing the firefly luciferase (27, 56). The BV^{CAR}GFP MOI was kept constant (500 vp/cell), while Ad5Luc MOI varied in the mix (MOI, 0, 50, or 100 vp/cell). Control samples consisted of (i) BV^{CAR}GFP alone without Ad5Luc and (ii) nonpseudotyped BV-GFP at the same constant dose (500 vp/cell) mixed with increasing MOIs of Ad5Luc. A modest but significant increase of GFP expression was detected in MSCs transduced by BV-GFP in the presence of Ad5Luc, compared to that with BV-GFP alone (50%; Fig. 10d, unbound Ad5). A similar level of enhancing effect was observed with BV^{CAR}GFP mixed with Ad5Luc (Fig. 10d; BV^{CAR}GFP-bound Ad5) compared to BV^{CAR}GFP alone. This indicated that Ad5 had only a discrete positive effect on the cellular internalization of the BV-GFP vector and that this effect did not require a physical bond between the baculovirion and the adenovirion.

(iv) Role of penton base-RGD-integrin recognition. To determine the contribution of RGD-dependent integrins in cell transduction by BV^{CAR}-Ad5GFP complex, we generated another baculoviral-adenoviral complex using the Ad5EGD-GFP mutant instead of the Ad5GFP vector. Due to its RGD-to-EGD alteration at position 340 in the penton base, the Ad5EGD-GFP mutant vector failed to recognize RGD-dependent integrins (26, 37, 67, 83). However, since the penton base mutation could mask or bias possible effects of BV^{CAR} in the BV^{CAR}-Ad5EGD-GFP complex, we first analyzed the intrinsic infectivity of Ad5EGD-GFP in permissive cells, in comparison to that of control Ad5GFP.

Ad5EGD-GFP stocks showed a range of infectivity indices (PFU/vp ratio) slightly inferior to that of control Ad5GFP vector grown in parallel, e.g., 1:108 versus 1:48, respectively, for the samples used in the present study. Ad5-permissive HEK-293 cells were infected by Ad5EGD-GFP or Ad5GFP at

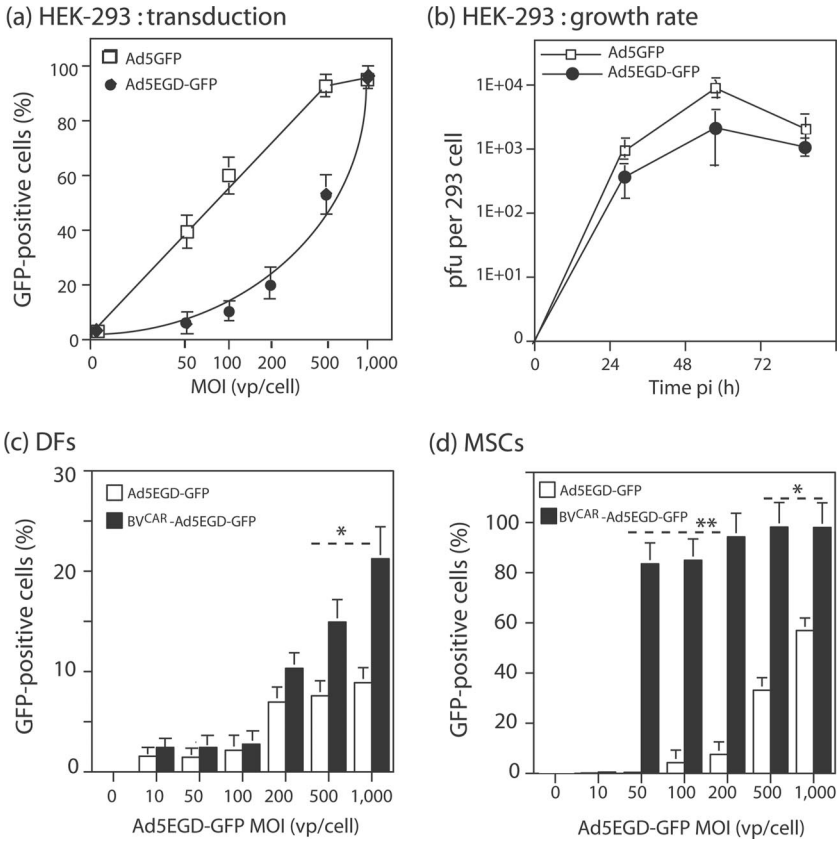

FIG. 11. Role of RGD-dependent integrins in BV^{CAR}-Ad5GFP-mediated transduction. (a) Efficiency of transduction of permissive cells by Ad5EGD-GFP mutant versus that by Ad5GFP. Aliquots of HEK-293 cells (1.75×10^5/well) were infected for 1 h with Ad5EGD-GFP or control vector Ad5GFP at different MOIs, as indicated on the *x* axis, and the percentage of GFP-positive cells was determined by flow cytometry at 48 h p.i. (means of three separate experiments ± SEMs). (b) Growth rate of Ad5EGD-GFP mutant versus that of Ad5GFP in permissive cells. Samples of 5×10^4 HEK-293 cells were infected at an MOI of 10 PFU/cell at 37°C for 1 h, rinsed once, and further incubated in culture medium at 37°C. Cells were harvested at 24, 48, and 72 h p.i. and lysed by freeze-thawing in 0.2 ml PBS, and titers of soluble supernatants were determined on HEK-293 cells. Titers were expressed as PFU/cell. (c and d) Efficiency of transduction by the BV^{CAR}-Ad5EGD-GFP complex. Dermal fibroblasts (DFs) (c) and MSCs (d) were transduced by Ad5EGD-GFP alone or a mixture of BV^{CAR} at a constant MOI (500 vp/cell) and Ad5EGD-GFP at increasing MOIs, as indicated on the *x* axis. The transduction efficiency was expressed as the percentage of GFP-positive cells, assayed by flow cytometry at 48 h p.i. (means of three separate experiments ± SEMs). *, $P < 0.05$; **, $P < 0.01$.

the same MOI (vp/cell), and the efficiency of infection and gene expression was determined by flow cytometric analysis of GFP-positive cells. The MOI required for 50% cell transduction (50% efficient transduction dose) was found to be 500 vp/cell for Ad5EGD-GFP, versus fivefold lower for Ad5GFP (50% efficient transduction dose = 100 vp/cell), and the maximum transduction was obtained at an MOI of 1,000 vp/cell for Ad5EGD-GFP, versus an MOI of 500 for Ad5GFP (Fig. 11a). These data showed that Ad5EGD-GFP infection was delayed compared to that by control vector Ad5GFP. Likewise, the growth rates were similar for the two vectors in HEK-293 cells, but the titer of infectious virus progeny recovered at 24, 48, and 72 h p.i. was three- to fourfold lower for Ad5EGD-GFP than for Ad5GFP (Fig. 11b). These data indicated that Ad5EGD-GFP was slightly but significantly impaired by its penton base mutation.

Taking into account the phenotype of Ad5EGD-GFP, we infected human dermal fibroblasts with Ad5EGD-GFP alone or BV^{CAR}-Ad5EGD-GFP complex at higher MOIs than those used previously with Ad5GFP and BV^{CAR}-Ad5GFP (Fig. 7 and 8). Of note, human dermal fibroblasts express alpha V integrins (21). Less than 10% of cells expressed GFP after transduction by Ad5EGD-GFP at an MOI of 1,000. With BV^{CAR}-Ad5EGD-GFP, however, a two- to threefold increase in transduction efficiency was observed at MOIs of 200 and higher (Fig. 11c). This moderate although significant augmentation was confirmed with other primary cells, MSCs. MSCs were transduced by BV^{CAR}-Ad5EGD-GFP with a 20-fold-higher efficiency at an MOI of 100 and a 10-fold-higher efficiency at an MOI of 200, compared to transduction with Ad5EGD-GFP alone (Fig. 11d). This implied that the integrity of penton base RGD motifs and their interaction with cellular integrins were not required for the BV^{CAR}-mediated augmentation of Ad5EGD-GFP transduction and that the BV^{CAR}-Ad5GFP complex could bypass the RGD-integrin endocytic pathway.

EM analysis of cell attachment and entry of BV^{CAR}-Ad5GFP complex into CAR-defective cells. CHO cells were incubated with BV^{CAR}-Ad5GFP complex for 1 h at 37°C, harvested at the end of this incubation period, fixed, and processed for EM

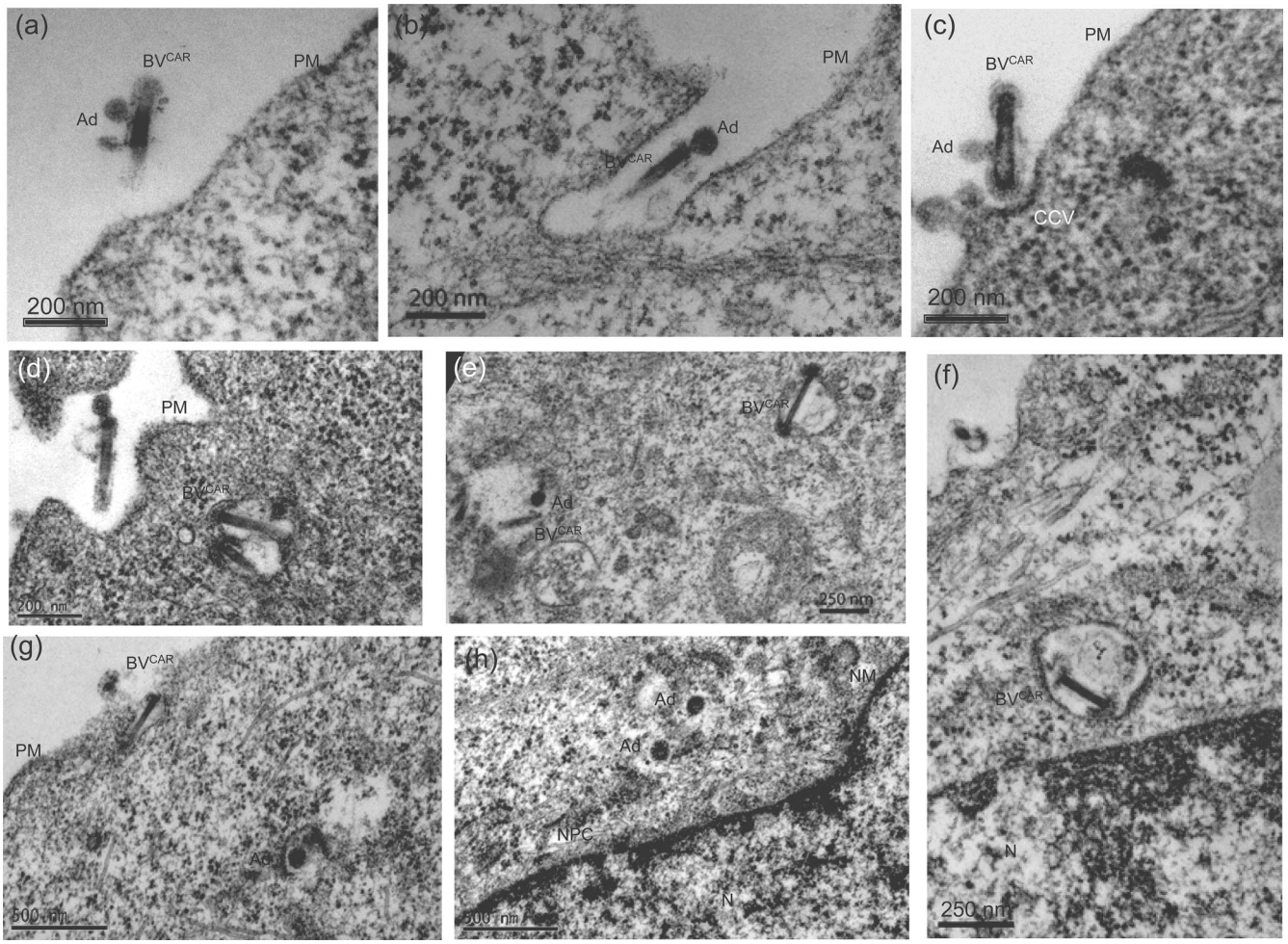

FIG. 12. EM analysis of the early steps of virus-cell interaction between BV^{CAR}-Ad5GFP complex and CAR-negative cells. Monolayers of CHO cells were incubated with BV^{CAR}-Ad5GFP (complex generated with an Ad5GFP-to-BV^{CAR} ratio of 1:25) for 1 h at 37°C, and cells were harvested and processed for EM analysis. Panels a to c show the steps of attachment of BV^{CAR}-Ad5GFP at the plasma membrane and formation of clathrin-coated vesicles (CCV). Panels d and e show coendocytosed virions of BV^{CAR} and Ad5GFP (Ad) within intracytoplasmic vesicles. In panel g, an adenovirion is seen in the process of vesicular escape. In panel h, two adenovirions are free within the cytoplasm, and electron-dense particles reminiscent of adenoviral cores are seen at the nuclear pore complex (NPC). Panel f shows an intravesicular BV^{CAR} nucleocapsid released from the baculoviral envelope. N, nucleus; PM, plasma membrane.

analysis. Complexes were seen at the cell surface, near or in close contact with the plasma membrane (Fig. 12a to d). At the point of BV^{CAR}-cell contact, a curvature of the plasma membrane with electron-dense material at its inner leaflet suggested the formation of a clathrin-coated pit (Fig. 12c), as previously reported (48). Coendocytosed baculovirions and adenovirions were observed within cytoplasmic vesicles (Fig. 12d and e). Adenovirions were occasionally seen in the process of vesicular escape with partial disruption of the endosomal membrane (Fig. 12g), or free within the cytoplasm, in the vicinity of nuclear pores (Fig. 12h). In contrast to Ad5 particles, baculoviral nucleocapsids were not observed within the cytoplasm and were still found within vesicles at 1 h p.i. (Fig. 12f). This suggested that adenovirions were released into the cytoplasm at a higher rate than were baculovirions. In none of the numerous cells examined did we observe a simultaneous endosomal escape of the two virions. This EM pattern was consistent with the relatively low rate of baculovirus release into the cytosol of mammalian cells (78) and supported the data for BV-bound and unbound Ad5Luc presented in Fig. 10d.

Biodistribution of BV^{CAR}-Ad5Luc complex in vivo in a mouse model. The preferential visceral localization of unmodified baculoviral vectors injected in the mouse tail vein has been reported to be, in decreasing order, heart, spleen, liver, kidney, lung, and brain (38). However, Ad5 vectors administered via the same way are in priority delivered to the liver (35, 61, 79, 81). It was therefore of interest to determine the viscerotropism of our BV^{CAR}-Ad5 complex and evaluate the respective influence of one or the other partner of the duo on the biodistribution of the complex in an animal model. To this aim, 5-week-old BALB/c nude mice received intravenously a bolus of 2×10^{10} vp of Ad5Luc or of BV^{CAR}-Ad5Luc complex (2×10^{10} vp of Ad5Luc and 3×10^{11} vp of BV^{CAR}, i.e., a ratio of BV^{CAR} to Ad5Luc vp of 15 to 1), and the level of luciferase expression was analyzed by noninvasive whole-body imaging at

days 2 and 4. The bioluminescent signal localized massively within the liver, and no qualitative difference could be detected between control mice receiving Ad5Luc alone and mice receiving the BV^{CAR}-Ad5Luc complex (not shown). Luciferase expression was then quantitatively assayed in different organs, and again the results showed that hepatic tissue was the preferential localization of both Ad5Luc alone and BV^{CAR}-Ad5Luc complex. In the other organs investigated, spleen, kidney, lung, brain, heart, and skeletal muscle, no significant difference in the levels of luciferase expression was found between Ad5Luc alone and the BV^{CAR}-Ad5Luc complex. The same organ distribution was observed when adenoviral genomes were quantitatively assayed using real-time quantitative PCR (data not shown). Of note, baculoviral genomes were recovered from the liver, as well as from the other tissues, and their relative distribution paralleled that of adenoviral genomes (data not shown). The change in tissue tropism of BV when complexed with Ad5 suggested that Ad5 carried the dominant determinants.

Influence of FX on BV^{CAR}-Ad5GFP-mediated transduction of CAR-negative cells in vitro. It has been shown recently that Ad5 hexon interacts with blood coagulation FX and to a lesser degree with FVII, FIX, and anticoagulant factor protein C (35, 61, 79, 81). The hexon-FX interaction is considered the major determinant of the preferential delivery of nonmodified Ad5 vectors to hepatocytes after in vivo administration. The next experiments were aimed at determining the possible role of FX in the hepatotropism of the BV^{CAR}-Ad5 complex, using an indirect, in vitro approach. Transduction of CHO cells by BV^{CAR}-Ad5GFP or Ad5GFP alone was performed in the presence or absence or FX. As expected from previous studies, a 20-fold increase in gene transfer efficiency was observed with Ad5GFP plus FX, compared to control Ad5GFP without FX: 42.6 ± 7.2 versus 1.9 ± 0.3 (mean $\pm$ standard error of the mean [SEM]; $n = 3$). However, when CHO cells were transduced with BV^{CAR}-Ad5GFP complex (generated with a suboptimal ratio of 10 BV^{CAR} to 1 Ad5GFP), no significant increase was observed: 26.1 ± 5.0 with FX versus 19.6 ± 1.5 without FX. This result suggested that FX had no direct effect on BV^{CAR}-Ad5GFP-mediated cell transduction in vitro.

DISCUSSION

The concept of BV display, i.e., exposing proteins or peptides of interest on the baculoviral envelope, is not novel and has been used to improve BV entry into different mammalian cell targets, including human cancer cells, by insertion of specific peptide ligands in the envelope glycoprotein gp64 (18, 39, 52–54, 75). This technology has also been used for immunization purposes (31, 32). The strategy described in the present study differed from conventional BV display methods in that it did not involve a gp64-fusion construct but consisted of the incorporation into the baculoviral envelope of a full-length glycoprotein normally exposed on the human cell plasma membrane and foreign to the virus. This fulfilled the criteria of virus pseudotyping. Such a pseudotyping of BV by, e.g., human hormone receptor (47) or vesicular stomatitis virus G (39), has been previously reported.

The originality of our strategy was to pseudotype BV with CAR (BV^{CAR}), the high-affinity receptor for Ad5 and several other Ad serotypes, to generate binary BV^{CAR}-Ad5 complexes via CAR-fiber knob interaction. BV^{CAR} was therefore used as a viral adapter to mediate cell entry of human Ad5 vector into Ad5-resistant cells. The rationale was based on two observations and implied two hypotheses. (i) It has been observed that BV has the capacity of entering a wide variety of cell types, including cells which are refractory to Ad5 infection, and to be internalized via a receptor-mediated pathway involving the early endosomal compartment (8, 32, 41, 73). (ii) The Ad5 fiber-CAR binding occurs with a high affinity, with a K_d (dissociation constant) range of 2 to 6 nM (27, 68, 85). We therefore hypothesized that (i) bridging Ad5 virions to BV^{CAR} via the strong interaction between adenoviral fiber and CAR glycoprotein inserted in the baculoviral envelope would result in the simultaneous cellular uptake of both Ad5 and BV^{CAR} into the same endocytic compartment and that (ii) the coendocytosed viruses would cooperate in the step of endosomolysis and contribute to a more efficient endosomal release and cell internalization.

We found that when Sf9 cells were infected with our recombinant BV expressing the human CAR glycoprotein under the control of the polyhedrin promoter, the BV progeny incorporated CAR molecules into the baculoviral envelope, resulting in a bona fide CAR-pseudotyped BV, abbreviated BV^{CAR}. EM analysis of BV^{CAR}-Ad5GFP complexes showed that the most frequent associations consisted of a stoichiometric ratio of one Ad5GFP per BV^{CAR} and less frequently two Ad5GFP per BV^{CAR}. EM observation of BV^{CAR}-Ad5GFP complexes and isolated BV^{CAR} virions immunogold labeled with anti-CAR or anti-gp64 antibodies revealed a gold grain topology different for gp64 and CAR molecules: gp64 localized at the head of the virus, whereas CAR molecules, free or engaged in bonds with Ad5 virions, preferentially localized along the stem.

We then exploited the capacity of BVs to transduce a wide repertoire of cell types. BV^{CAR} was used to piggyback Ad5GFP vector into cells which do not express CAR and were nonpermissive or poorly permissive to Ad5. We found that the transduction enhancement of CHO and MM39 cells using the BV^{CAR}-Ad5GFP complex was on the order of 30- to 40-fold, compared to Ad5GFP alone. For three human cancer cell lines, RD, SKOV3, and SKBR3, a significant augmentation of gene delivery (3- to 10-fold) was observed with BV^{CAR}-Ad5GFP. In the case of primary cells, dermal fibroblasts, synoviocytes, and MSCs, BV^{CAR}-Ad5GFP-mediated transduction increased by 1 order of magnitude and, more importantly, at a significantly low Ad5GFP input (MOI of 20 vp/cell). For cells of myeloid origin such as PBMCs and monocyte-derived DCs, the increase in BV^{CAR}-Ad5GFP-mediated transduction was less pronounced (only twofold) and observed only at high Ad5 vector doses of MOIs of 1,000 and 500, respectively. Not surprisingly, PBMCs and DCs have not been reported in the literature to efficiently internalize BVs.

We showed that the mechanism of augmentation of cell transduction of primary cells (e.g., dermal fibroblasts and synoviocytes) by BV^{CAR}-Ad5GFP in vitro, compared to Ad5GFP alone, required (i) the interaction of adenoviral fibers with CAR molecules inserted in the baculoviral envelope and (ii) the cell attachment of the BV^{CAR} partner via its gp64 peplomer; (iii) however, it did not depend on the interaction of penton base RGD motifs of the Ad5GFP partner with cellular

integrins; (iv) kinetic analysis of the virus-cell binding reaction showed that the presence of BV^{CAR} in the complex was beneficial to Ad5GFP, in terms of number of cell-bound virions and rate of cell attachment; (v) however, there was little reciprocity, as the benefit obtained by BV^{CAR} from its Ad5GFP partner in terms of rate of endosomal escape and cell internalization was modest.

Our data with control nonpseudotyped baculoviral vector BV-GFP, and BV-bound or unbound Ad5 vector, suggested that the helper function of BV^{CAR} toward Ad5GFP vector (2- to 40-fold-increased transduction in the various cell types tested) was much higher than that in the opposite scenario, when Ad5 was used as the helper of BV^{CAR}-GFP (only 50%). We assume that this was due to the mechanisms of vesicular escape, which differ for the two viruses. Both BVs and subgroup C Ads are endocytosed into early endosomes but are released into the cytosol by different mechanisms: Ads rapidly escape from endosomes by endosomolysis (30), while BVs use membrane fusion between baculoviral envelope glycoprotein and the endosomal membrane (32, 70). Our data indicated that the cell entry pathway and rate of endosomal escape of BV^{CAR} via gp64-mediated membrane fusion were not greatly affected by the presence of its Ad5GFP partner in the BV^{CAR}-Ad5GFP complex. However, both partners of the BV^{CAR}-Ad5GFP duo played their own part in one or the other step of the cell entry pathway, and cellular transduction benefited from the ensemble.

In vivo, after intravascular administration in BALB/c nude mice, the biodistribution of BV^{CAR}-Ad5Luc complex was unchanged compared to that of Ad5Luc alone, and the liver remained the preferred destination of the viral duo, as observed for unmodified Ad5 vectors in many laboratories (35, 61, 79, 81). Unmodified baculoviral vectors injected in the mouse tail vein also have intrinsic hepatotropism (6) but localize in smaller amounts in the liver, compared to heart and spleen (38). This suggested that Ad5 played the dominant role in the vector duo. Our in vitro experiments showed that BV^{CAR}-Ad5GFP-mediated transduction of CAR-negative cells was insensitive to blood coagulation FX and FX-hexon interaction (35, 61, 79, 81), in contrast to transduction by Ad5GFP alone, which was drastically enhanced in the presence of FX.

In conclusion, the advantages of using CAR-pseudotyped BV as a carrier of Ad5 vector(s) are multiple. (i) Many cells which are poorly permissive to Ad5 can be transduced at high MOIs of Ad5 vector, and up to 10^4 to 10^5 particles per cell are necessary to obtain a minimal level of transgene expression. Such high MOIs are hardly compatible with the cell physiology, and intrinsic vector cytotoxicity is likely to interfere with the biological function(s) of the transgene product(s). By comparison, our BV^{CAR}-Ad5 vector complex efficiently transduced Ad5-refractory cells at MOIs of 10 to 20. (ii) In the same line of arguments, Ad5 has an early cytopathic and cell-detaching effect, and the cell-detaching effect has been assigned to one of the major capsid proteins of incoming virions, the penton base and its integrin-binding motif RGD (4, 36, 37, 62). Results with penton base EGD mutant Ad5 suggested that our BV^{CAR}-Ad5 vector complex could bypass the RGD-integrin endocytic pathway. (iii) It is relatively easy to insert a gene of interest in the E1-deleted region of Ad5, and many commercial kits are available to generate recombinant Ad5. It is less easy, however, to modify the adenoviral capsid so as to redirect the Ad5 vector to a desired cell target via cell-specific ligands, while respecting the viability and the productivity of capsid-modified vectors (51). Our strategy of using BV^{CAR} as a macromolecular adapter of Ad5 vector, therefore, represents an alternative to hazardous Ad capsid modifications.

(iv) BV^{CAR}, and a fortiori our BV^{CAR}-Ad5 vector complex, could be redirected to cell targets by insertion of specific peptides or proteins in the envelope glycoprotein gp64 (18, 39, 52–54, 75). (v) Considering the last point (iv), it might be argued that there would be no need for a BV^{CAR}-Ad5 vector complex and that a recombinant BV vector expressing the gene of interest under the required promoter (31) and displaying a cell-targeting ligand would be sufficient for gene delivery to human cells nonpermissive to Ad5. However, our data indicated that our BV^{CAR}-Ad5GFP duo was significantly more efficient than BV^{CAR}-GFP alone in cell transduction of vertebrate cells. (vi) Given the possibility of transducing Ad-refractory cells belonging to the immune system by our BV^{CAR}-Ad5 vector complex, one could envisage delivering oncolytic Ads to tumors via cell carriers with specificity toward tumor cells. (vii) Although results of in vitro experiments could hardly be extrapolated to in vivo situations, our preliminary data suggested that the hepatotropism of the BV^{CAR}-Ad5GFP complex was independent of Ad5 hexon-FX interaction. (viii) Lastly, our system of coupling two viruses which are both vectors of gene transfer also offers the possibility of expressing several transgenes within the same target cell, while limiting the risk of interference between transgenes and promoters carried by a single recombinant genome.

ACKNOWLEDGMENTS

This work was supported by the French Cystic Fibrosis Foundation (Vaincre La Mucoviscidose, VLM contracts TG-0702 and TG-0801), the Centre National Recherche Scientifique (CNRS), the University of Lyon I, and the Hospices Civils de Lyon (HCL). O.G. was financially supported by a postdoctoral fellowship from VLM. K.K. was supported by the AMS-IRD URI-174 PHPT Franco-Thai Cooperation Program for High Education and Research and the Thai Higher Education Program. S.-S.H. is an INSERM scientist and the recipient of a Contrat d'Interface HCL-INSERM.

We are deeply grateful to Gérard Devauchelle (CNRS, St. Christolles-Ales, France) for his valuable advice on BV technology, to Kerstin Sollerbrant (Karolinska Institutet, Stockholm, Sweden) for her gift of plasmid pcDNA-hCAR1, to Norman Maitland (University of York Heslington, York, United Kingdom) for the baculoviral clone expressing GFP, to Frank Graham (University of Ontario, Hamilton, Ontario, Canada) for the Ad5Luc3 vector, and to Silvio Hemmi (University of Zurich, Zurich, Switzerland) for the monoclonal anti-CAR antibody. We also thank Elisabeth Errazuriz (Centre Commun d'Imagerie de Laennec), for her help with our electron microscopic studies; Blandine Deux, Olivier Peyruchaud, and Philippe Clezardin (INSERM U-664, Laennec School of Medicine, Lyon) for their significant contribution to our animal experiments; Gaelle Gonzalez for her valuable assistance in our quantitative PCR analyses; and Cathy Berthet for her efficient secretarial aid.

REFERENCES

1. **Ayres, M. D., S. C. Howard, J. Kuzio, M. Lopez-Ferber, and R. D. Possee.** 1994. The complete DNA sequence of *Autographa californica* nuclear polyhedrosis virus. Virology **202:**586–605.
2. **Belousova, N., G. Mikheeva, J. Gelovani, and V. Krasnykh.** 2008. Modification of adenovirus capsid with a designed protein ligand yields a gene vector targeted to a major molecular marker of cancer. J. Virol. **82:**630–637.
3. **Bergelson, J. M., J. A. Cunningham, G. Droguett, E. A. Kurt-Jones, A. Krithivas, J. S. Hong, M. S. Horwitz, R. L. Crowell, and R. W. Finberg.** 1997.

Isolation of a common receptor for Coxsackie B viruses and adenoviruses 2 and 5. Science **275:**1320–1323.
4. **Boudin, M.-L., M. Moncany, J.-C. D'Halluin, and P. Boulanger.** 1979. Isolation and characterization of adenovirus type 2 vertex capsomer (penton base). Virology **92:**125–138.
5. **Boulanger, P., and F. Puvion.** 1973. Large-scale preparation of soluble adenovirus hexon, penton and fiber antigens in highly purified form. Eur. J. Biochem. **39:**37–42.
6. **Boyce, F. M., and N. L. Bucher.** 1996. Baculovirus-mediated gene transfer into mammalian cells. Proc. Natl. Acad. Sci. USA **93:**2348–2352.
7. **Chorny, M., I. Fishbein, I. S. Alferiev, O. Nyanguile, R. Gaster, and R. J. Levy.** 2006. Adenoviral gene vector tethering to nanoparticle surfaces results in receptor-independent cell entry and increased transgene expression. Mol. Ther. **14:**382–391.
8. **Chuang, C.-K., L.-Y. Sung, S.-M. Hwang, W.-H. Lo, H.-C. Chen, and Y.-C. Hu.** 2007. Baculovirus as a new gene delivery vector for stem cell engineering and bone tissue engineering. Gene Ther. **14:**1417–1424.
9. **Corjon, S., A. Wortmann, T. Engler, N. van Rooijen, S. Kochanek, and F. Kreppel.** 2008. Targeting of adenovirus vectors to the LRP receptor family with the high-affinity ligand RAP via combined genetic and chemical modification of the pIX capsomer. Mol. Ther. **16:**1813–1824.
10. **DaFonseca, S., A. Blommaert, P. Coric, S. S. Hong, S. Bouaziz, and P. Boulanger.** 2007. The 3-O-(3′,3′-dimethylsuccinyl) derivative of betulinic acid (DSB) inhibits the assembly of virus-like particles in HIV-1 Gag precursor-expressing cells. Antivir. Ther. **12:**1185–1203.
11. **Dechecchi, M. C., P. Melotti, A. Bonizzato, M. Santacatterina, M. Chilosi, and G. Cabrini.** 2001. Heparan sulfate glycosaminoglycans are receptors sufficient to mediate the initial binding of adenovirus types 2 and 5. J. Virol. **75:**8772–8780.
12. **Dechecchi, M. C., A. Tamanini, A. Bonizzato, and G. Cabrini.** 2000. Heparan sulfate glycosaminoglycans are involved in adenovirus type 5 and 2-host cell interactions. Virology **268:**382–390.
13. **Franqueville, L., P. Henning, M. K. Magnusson, E. Vigne, G. Schoehn, M. E. Blair-Zajdel, N. Habib, L. Lindholm, G. E. Blair, S. S. Hong, and P. Boulanger.** 2008. Protein crystals in adenovirus type 5-infected cells: requirements for intranuclear crystallogenesis, structural and functional analysis. PLoS One **3:**e2894.
14. **Gaden, F., L. Franqueville, S. S. Hong, V. Legrand, C. Figarella, and P. Boulanger.** 2002. Mechanism of restriction of normal and cystic fibrosis transmembrane conductance regulator-deficient human tracheal gland cells to adenovirus (Ad) infection and Ad-mediated gene transfer. Am. J. Respir. Cell Mol. Biol. **27:**628–640.
15. **Gaden, F., L. Franqueville, M. K. Magnusson, S. S. Hong, M. D. Merten, L. Lindholm, and P. Boulanger.** 2004. Gene transduction and cell entry pathway of fiber-modified adenovirus type 5 vectors carrying novel endocytic peptide ligands selected on human tracheal glandular cells. J. Virol. **78:**7227–7247.
16. **Goujon, C., L. Jarrosson-Wuilleme, J. Bernaud, D. Rigal, J. L. Darlix, and A. Cimarelli.** 2003. Heterologous human immunodeficiency virus type 1 lentiviral vectors packaging a simian immunodeficiency virus-derived genome display a specific postentry transduction defect in dendritic cells. J. Virol. **77:**9295–9304.
17. **Granio, O., C. Norez, K. J. D. Asbourne Excoffon, P. Karpp, M. Lusky, F. Becq, P. Boulanger, J. Zabner, and S. S. Hong.** 2007. Cellular localization and activity of GFP-tagged CFTR transduced by adenovirus in CFTR-deficient cells. Am. J. Respir. Cell Mol. Biol. **37:**631–639.
18. **Guibinga, G. H., and T. Friedmann.** 2005. Baculovirus gp64-pseudotyped HIV-based lentivirus vectors are stabilized against complement inactivation by codisplay of decay accelerating factor (DAF) or of a gp64-DAF fusion protein. Mol. Ther. **11:**645–651.
19. **Hemmi, S., R. Geertsen, A. Mezzacasa, I. Peter, and R. Dummer.** 1998. The presence of human coxsackievirus and adenovirus receptor is associated with efficient adenovirus-mediated transgene expression in human melanoma cell cultures. Hum. Gene Ther. **9:**2363–2373.
20. **Henning, P., M. K. Magnusson, E. Gunneriusson, S. S. Hong, P. Boulanger, P. A. Nygren, and L. Lindholm.** 2002. Genetic modification of adenovirus 5 tropism by a novel class of ligands based on a three-helix bundle scaffold derived from staphylococcal protein A. Hum. Gene Ther. **13:**1427–1439.
21. **Hidaka, C., E. Milano, P. L. Leopold, J. M. Bergelson, N. R. Hackett, R. W. Finberg, T. J. Wickham, I. Kovesdi, P. Roelvink, and R. G. Crystal.** 1999. CAR-dependent and CAR-independent pathways of adenovirus vector-mediated gene transfer and expression in human fibroblasts. J. Clin. Investig. **103:**579–587.
22. **Hofmann, C., V. Sandig, G. Jennings, M. Rudolph, P. Schlag, and M. Strauss.** 1995. Efficient gene transfer into human hepatocytes by baculovirus vectors. Proc. Natl. Acad. Sci. USA **92:**10099–10103.
23. **Hofmann, C., and M. Strauss.** 1998. Baculovirus-mediated gene transfer in the presence of human serum or blood facilitated by inhibition of the complement system. Gene Ther. **5:**531–536.
24. **Honda, T., H. Saitoh, M. Masuko, T. Katagiri-Abe, K. Tominaga, I. Kozakai, K. Kobayashi, T. Kumanishi, Y. G. Watanabe, S. Odani, and R. Kuwano.** 2000. The coxsackievirus-adenovirus receptor protein as a cell adhesion molecule in the developing mouse brain. Brain Res. Mol. Brain Res. **77:**19–28.
25. **Hong, S. S., A. Galaup, R. Peytavi, N. Chazal, and P. Boulanger.** 1999. Enhancement of adenovirus-mediated gene delivery by use of an oligopeptide with dual binding specificity. Hum. Gene Ther. **10:**2577–2586.
26. **Hong, S. S., B. Gay, L. Karayan, M. C. Dabauvalle, and P. Boulanger.** 1999. Cellular uptake and nuclear delivery of recombinant adenovirus penton base. Virology **262:**163–177.
27. **Hong, S. S., L. Karayan, J. Tournier, D. T. Curiel, and P. Boulanger.** 1997. Adenovirus type 5 fiber knob binds to MHC class I alpha2 domain at the surface of human epithelial and B lymphoblastoid cells. EMBO J. **16:**2294–2306.
28. **Hong, S. S., M. K. Magnusson, P. Henning, L. Lindholm, and P. Boulanger.** 2003. Adenovirus stripping: a versatile method to generate adenovirus vectors with new cell target specificity. Mol. Ther. **7:**692–699.
29. **Hong, S. S., E. Szolajska, G. Schoehn, L. Franqueville, S. Myhre, L. Lindholm, R. W. Ruigrok, P. Boulanger, and J. Chroboczek.** 2005. The 100K-chaperone protein from adenovirus serotype 2 (subgroup C) assists in trimerization and nuclear localization of hexons from subgroups C and B adenoviruses. J. Mol. Biol. **352:**125–138.
30. **Horwitz, M. S.** 2001. Adenoviruses, p. 2301–2326. *In* D. M. Knipe, P. M. Howley, D. E. Griffin, R. A. Lamb, M. A. Martin, B. Roizman, and S. E. Straus (ed.), Fields virology, 4th ed. Lippincott Williams & Wilkins, Philadelphia, PA.
31. **Hu, Y. C.** 2008. Baculoviral vectors for gene delivery: a review. Curr. Gene Ther. **8:**54–65.
32. **Hu, Y. C.** 2006. Baculovirus vectors for gene therapy. Adv. Virus Res. **68:**287–320.
33. **Hüser, A., M. Rudolph, and C. Hofmann.** 2001. Incorporation of decay-accelerating factor into the baculovirus envelope generates complement-resistant gene transfer vectors. Nat. Biotechnol. **19:**451–455.
34. **Huvent, I., S. S. Hong, C. Fournier, B. Gay, J. Tournier, C. Carriere, M. Courcoul, R. Vigne, B. Spire, and P. Boulanger.** 1998. Interaction and coencapsidation of HIV-1 Vif and Gag recombinant proteins. J. Gen. Virol. **79:**1069–1081.
35. **Kalyuzhniy, O., N. C. Di Paolo, M. Silvestry, S. E. Hofherr, M. A. Barry, P. L. Stewart, and D. M. Shayakhmetov.** 2008. Adenovirus serotype 5 hexon is critical for virus infection of hepatocytes in vivo. Proc. Natl. Acad. Sci. USA **105:**5483–5488.
36. **Karayan, L., B. Gay, J. Gerfaux, and P. Boulanger.** 1994. Oligomerization of recombinant penton base of adenovirus type 2 and its assembly with fiber in baculovirus-infected cells. Virology **202:**782–795.
37. **Karayan, L., S. S. Hong, B. Gay, J. Tournier, A. D. d'Angeac, and P. Boulanger.** 1997. Structural and functional determinants in adenovirus type 2 penton base recombinant protein. J. Virol. **71:**8678–8689.
38. **Kim, Y.-K., I.-K. Park, H.-L. Jiang, J.-Y. Choi, Y.-H. Je, H. Jin, H.-W. Kim, M.-H. Cho, and C.-S. Cho.** 2006. Regulation of transduction efficiency by pegylation of baculovirus vector in vitro and in vivo. J. Biotechnol. **125:**104–109.
39. **Kitagawa, Y., H. Tani, C. K. Limn, T. M. Matsunaga, K. Moriishi, and Y. Matsuura.** 2005. Ligand-directed gene targeting to mammalian cells by pseudotype baculoviruses. J. Virol. **79:**3639–3652.
40. **Korokhov, N., G. Mikheeva, A. Krendelshchikov, N. Belousova, V. Simonenko, V. Krendelshchikova, A. Pereboev, A. Kotov, O. Kotova, P. L. Triozzi, W. A. Aldrich, J. T. Douglas, K. M. Lo, P. T. Banerjee, S. D. Gillies, D. T. Curiel, and V. Krasnykh.** 2003. Targeting of adenovirus via genetic modification of the viral capsid combined with a protein bridge. J. Virol. **77:**12931–12940.
41. **Kost, T. A., and J. P. Condreay.** 2002. Recombinant baculoviruses as mammalian cell gene-delivery vectors. Trends Biotechnol. **20:**173–180.
42. **Kreppel, F., J. Gackowski, E. Schmidt, and S. Kochanek.** 2005. Combined genetic and chemical capsid modifications enabled flexible and efficient de- and retargeting of adenovirus vectors. Mol. Ther. **12:**107–117.
43. **Law, L. K., and B. L. Davidson.** 2005. What does it take to bind CAR? Mol. Ther. **12:**599–609.
44. **Lehtolainen, P., K. Tyynelä, J. Kannasto, K. J. Airenne, and S. Ylä-Herttuala.** 2002. Baculoviruses exhibit restricted cell type specificity in rat brain: a comparison of baculovirus- and adenovirus-mediated intracerebral gene transfer in vivo. Gene Ther. **9:**1693–1699.
45. **Leisy, D. J., T. D. Lewis, J.-A. C. Leong, and G. F. Rohrmann.** 2003. Transduction of cultured fish cells with recombinant baculoviruses. J. Gen. Virol. **84:**1173–1178.
46. **Li, Y. P., S. Paczesny, E. Lauret, S. Poirault, P. Bordigoni, F. Mekhloufi, O. Hequet, Y. Bertrand, J. P. Ou-Yang, J. F. Stoltz, P. Miossec, and A. Eljaafari.** 2008. Human mesenchymal stem cells license adult CD34+ hemopoietic progenitor cells to differentiate into regulatory dendritic cells through activation of the Notch pathway. J. Immunol. **180:**1598–1608.
47. **Loisel, T. P., H. Ansanay, S. St.-Onge, B. Gay, P. Boulanger, A. D. Strosberg, S. Marullo, and M. Bouvier.** 1997. Recovery of homogeneous and functional beta 2-adrenergic receptors from extracellular baculovirus particles. Nat. Biotechnol. **15:**1300–1304.
48. **Long, G., X. Pan, R. Kormelink, and J. M. Vlak.** 2006. Functional entry of

baculovirus into insect and mammalian cells is dependent on clathrin-mediated endocytosis. J. Virol. **80:**8830–8833.
49. **Magnusson, M. K., P. Henning, S. Myhre, M. Wikman, T. G. Uil, M. Friedman, K. M. Andersson, S. S. Hong, R. C. Hoeben, N. A. Habib, S. Stahl, P. Boulanger, and L. Lindholm.** 2007. Adenovirus 5 vector genetically retargeted by an Affibody molecule with specificity for tumor antigen HER2/neu. Cancer Gene Ther. **14:**468–479.
50. **Magnusson, M. K., S. S. Hong, P. Boulanger, and L. Lindholm.** 2001. Genetic retargeting of adenovirus: novel strategy employing "deknobbing" of the fiber. J. Virol. **75:**7280–7289.
51. **Magnusson, M. K., S. S. Hong, P. Henning, P. Boulanger, and L. Lindholm.** 2002. Genetic retargeting of adenovirus vectors: functionality of targeting ligands and their influence on virus viability. J. Gene Med. **4:**356–370.
52. **Mäkelä, A. R., J. Enbäck, J. P. Laakkonen, M. Vihinen-Ranta, P. Laakkonen, and C. Oker-Blom.** 2008. Tumor targeting of baculovirus displaying a lymphatic homing peptide. J. Gene Med. **10:**1019–1031.
53. **Mäkelä, A. R., H. Matilainen, D. J. White, E. Ruoslahti, and C. Oker-Blom.** 2006. Enhanced baculovirus-mediated transduction of human cancer cells by tumor-homing peptides. J. Virol. **80:**6603–6611.
54. **Mäkelä, A. R., and C. Oker-Blom.** 2006. Baculovirus display: a multifunctional technology for gene delivery and eukaryotic library development. Adv. Virus Res. **68:**91–112.
55. **Matthews, D. A., and W. C. Russell.** 1994. Adenovirus protein-protein interactions: hexon and protein VI. J. Gen. Virol. **75:**3365–3374.
56. **Mittal, S. K., M. R. McDermott, D. C. Johnson, L. Prevec, and F. L. Graham.** 1993. Monitoring foreign gene expression by a human adenovirus-based vector using the firefly luciferase gene as a reporter. Virus Res. **28:**67–90.
57. **Mizuguchi, H., and T. Hayakawa.** 2002. Adenovirus vectors containing chimeric type 5 and type 35 fiber proteins exhibit altered and expanded tropism and increase the size limit of foreign genes. Gene **285:**69–77.
58. **Molinier-Frenkel, V., R. Lengagne, F. Gaden, S. S. Hong, J. Choppin, H. Gahery-Segard, P. Boulanger, and J. G. Guillet.** 2002. Adenovirus hexon protein is a potent adjuvant for activation of a cellular immune response. J. Virol. **76:**127–135.
59. **Monsma, S. A., A. G. Oomens, and G. W. Blissard.** 1996. The GP64 envelope fusion protein is an essential baculovirus protein required for cell-to-cell transmission of infection. J. Virol. **70:**4607–4616.
60. **Novelli, A., and P. Boulanger.** 1991. Deletion analysis of functional domains in baculovirus-expressed adenovirus type 2 fiber. Virology **185:**365–376.
61. **Parker, A. L., S. N. Waddington, C. G. Nicol, D. M. Shayakhmetov, S. M. Buckley, L. Denby, G. Kemball-Cook, S. Ni, A. Lieber, J. H. McVey, S. A. Nicklin, and A. H. Baker.** 2006. Multiple vitamin K-dependent coagulation zymogens promote adenovirus-mediated delivery to hepatocytes. Blood **108:**2554–2561.
62. **Pereira, H. G.** 1958. A protein factor responsible for the early cytopathic effect of adenoviruses. Virology **6:**601–611.
63. **Peyruchaud, O., C. M. Serre, R. NicAmhlaoibh, P. Fournier, and P. Clezardin.** 2003. Angiostatin inhibits bone metastasis formation in nude mice through a direct anti-osteoclastic activity. J. Biol. Chem. **278:**45826–45832.
64. **Russell, W. C.** 2009. Adenoviruses: update on structure and function. J. Gen. Virol. **90:**1–20.
65. **Russell, W. C.** 2000. Update on adenovirus and its vectors. J. Gen. Virol. **81:**2573–2604.
66. **Russell, W. C., G. Patel, B. Precious, I. Sharp, and P. S. Gardner.** 1981. Monoclonal antibodies against adenovirus type 5: preparation and preliminary characterization. J. Gen. Virol. **56:**393–408.
67. **Salone, B., Y. Martina, S. Piersanti, E. Cundari, G. Cherubini, L. Franqueville, C. M. Failla, P. Boulanger, and I. Saggio.** 2003. Integrin $\alpha 3\beta 1$ is an alternative receptor for adenovirus serotype 5. J. Virol. **77:**13448–13454.
68. **Santis, G., V. Legrand, S. S. Hong, E. Davison, I. Kirby, J. L. Imler, R. W. Finberg, J. M. Bergelson, M. Mehtali, and P. Boulanger.** 1999. Molecular determinants of adenovirus serotype 5 fibre binding to its cellular receptor CAR. J. Gen. Virol. **80:**1519–1527.
69. **Sarkis, C., C. Serguera, S. Petres, D. Buchet, J.-L. Ridet, L. Edelman, and J. Mallet.** 2000. Efficient transduction of neural cells in vitro and in vivo by a baculovirus-derived vector. Proc. Natl. Acad. Sci. USA **97:**14638–14643.
70. **Slack, J., and B. M. Arif.** 2007. The baculoviruses occlusion-derived virus: virion structure and function. Adv. Virus Res. **69:**99–165.
71. **Sollerbrant, K., E. Raschperger, M. Mirza, U. Engstrom, L. Philipson, P. O. Ljungdahl, and R. F. Pettersson.** 2003. The Coxsackievirus and adenovirus receptor (CAR) forms a complex with the PDZ domain-containing protein ligand-of-numb protein-X (LNX). J. Biol. Chem. **278:**7439–7444.
72. **Songa, J., C. Lianga, and X. Chen.** 2006. Transduction of avian cells with recombinant baculovirus. J. Virol. Methods **135:**157–162.
73. **Stanbridge, L. J., V. Dussupt, and N. J. Maitland.** 2003. Baculoviruses as vectors for gene therapy against human prostate cancer. J. Biomed. Biotechnol. **2003:**79–91.
74. **Takayama, K., P. N. Reynolds, J. J. Short, Y. Kawakami, Y. Adachi, J. N. Glasgow, M. G. Rots, V. Krasnykh, J. T. Douglas, and D. T. Curiel.** 2003. A mosaic adenovirus possessing serotype Ad5 and serotype Ad3 knobs exhibits expanded tropism. Virology **309:**282–293.
75. **Tani, H., M. Nishijima, H. Ushijima, T. Miyamura, and Y. Matsuura.** 2001. Characterization of cell-surface determinants important for baculovirus infection. Virology **279:**343–353.
76. **Toh, M. L., S. S. Hong, F. van de Loo, L. Franqueville, L. Lindholm, W. van den Berg, P. Boulanger, and P. Miossec.** 2005. Enhancement of adenovirus-mediated gene delivery to rheumatoid arthritis synoviocytes and synovium by fiber modifications: role of arginine-glycine-aspartic acid (RGD)- and non-RGD-binding integrins. J. Immunol. **175:**7687–7698.
77. **Tomko, R. P., R. Xu, and L. Philipson.** 1997. HCAR and MCAR: the human and mouse cellular receptors for subgroup C adenoviruses and group B coxsackieviruses. Proc. Natl. Acad. Sci. USA **94:**3352–3356.
78. **van Loo, N. D., E. Fortunati, E. Ehlert, M. Rabelink, F. Grosveld, and B. J. Scholte.** 2001. Baculovirus infection of nondividing mammalian cells: mechanisms of entry and nuclear transport of capsids. J. Virol. **75:**961–970.
79. **Vigant, F., D. Descamps, B. Jullienne, S. Esselin, E. Connault, P. Opolon, T. Tordjmann, E. Vigne, M. Perricaudet, and K. Benihoud.** 2008. Substitution of hexon hypervariable region 5 of adenovirus serotype 5 abrogates blood factor binding and limits gene transfer to liver. Mol. Ther. **16:**1474–1480.
80. **Volkman, L. E., M. D. Summers, and C.-H. Hsieh.** 1976. Occluded and nonoccluded nuclear polyhedrosis virus grown in *Trichoplusia ni*: comparative neutralization, comparative infectivity, and in vitro growth studies. J. Virol. **19:**820–832.
81. **Waddington, S. N., J. H. McVey, D. Bhella, A. L. Parker, K. Barker, H. Atoda, R. Pink, S. M. Buckley, J. A. Greig, L. Denby, J. Custers, T. Morita, I. M. Francischetti, R. Q. Monteiro, D. H. Barouch, N. van Rooijen, C. Napoli, M. J. Havenga, S. A. Nicklin, and A. Baker.** 2008. Adenovirus serotype 5 hexon mediates liver gene transfer. Cell **132:**397–409.
82. **Walters, R. W., P. Freimuth, T. O. Moninger, I. Ganske, J. Zabner, and M. J. Welsh.** 2002. Adenovirus fiber disrupts CAR-mediated intercellular adhesion allowing virus escape. Cell **110:**789–799.
83. **Waszak, P., L. Franqueville, M.-L. Franco-Motoya, M. Rosa-Calatrava, O. Boucherat, L. Lindholm, C. Delacourt, and P. Boulanger.** 2007. Toxicity of fiber- and penton base-modified adenovirus type 5 vectors on lung development in newborn rats. Mol. Ther. **15:**2008–2016.
84. **Wickham, T. J., E. J. Filardo, D. A. Cheresh, and G. R. Nemerow.** 1994. Integrin alpha-v beta-5 selectively promotes adenovirus mediated cell membrane permeabilization. J. Cell Biol. **127:**257–264.
85. **Wickham, T. J., P. Mathias, D. A. Cheresh, and G. R. Nemerow.** 1993. Integrins alpha-v beta-3 and alpha-v beta-5 promote adenovirus internalization but not virus attachment. Cell **73:**309–319.
86. **Zabner, J., M. Chillon, T. Grunst, T. O. Moninger, B. L. Davidson, R. Gregory, and D. Armentano.** 1999. A chimeric type 2 adenovirus vector with a type 17 fiber enhances gene transfer to human airway epithelia. J. Virol. **73:**8689–8695.